EFFECTIVE BIOSORPTION OF PHOSPHATE IONS FROM AQUEOUS SOLUTION USING Fe(III)-LOADED CARBOXYL FUNCTIONALIZED BANANA PEELS

A Dissertation

Submitted as a Partial Fulfilment for the Requirement of Master Degree of Science in Chemistry

BY

PUKAR BHATTARAI

Symbol No: 1895/076

T.U. Regd No: 5-2-37-2024-2012

AMRIT CAMPUS

INSTITUTE OF SCIENCE AND TECHNOLOGY

TRIBHUVAN UNIVERSITY

LAINCHAUR, KATHMANDU

NEPAL

JULY 2023

CERTIFICATE OF APPROVAL

This dissertation work, submitted by Pukar Bhattarai and entitled **"Effective Biosorption of Phosphate Ions from Aqueous Solution Using Fe(III)-Loaded Carboxyl Functionalized Banana Peels,"** was carried out at Amrit Campus, Tribhuvan University, Nepal, under the supervision of Assistant Professor **Dr. Ram Lochan Aryal** & co-supervisor **Mr. Naresh Prashad Pant**. It is being submitted in partial fulfilment of the requirements for a Master of Science (M. Sc.).

.....

Asst. Prof. Dr. Ram Lochan Aryal

Supervisor

Amrit Campus, Lainchaur

Tribhuvan University, Kathmandu

Nepal

.....

Mr. Naresh Prashad Pant

Co-supervisor

Amrit Campus, Lainchaur

Tribhuvan University, Kathmandu

Nepal

.....

Asst. Prof. Dr. Hari Paudyal

External Examiner

Central Department of Chemistry

Tribhuvan University, Kirtipur

Kathmandu, Nepal

.....

Asst. Prof. Dr. Deval Prasad Bhattarai

Internal Examiner

Amrit Campus, Lainchaur

Tribhuvan University, Kathmandu

Nepal

Tribhuvan University
Amrit Campus
Department of Chemistry

.....

Assoc. Prof. Kanchan Sharma

Head of Department

Amrit Campus, Lainchaur

Tribhuvan University, Kathmandu

Nepal

.....

Assoc. Prof. Dr. Bhusan Shakya

M.Sc Program Coordinator

Amrit Campus, Lainchaur

Tribhuvan University, Kathmandu

Nepal

Date: Aug - 3, 2023

RECOMMENDATION LETTER

This is to certify that the thesis entitled **"Effective Biosorption of Phosphate Ions from Aqueous Solution Using Fe(III)-Loaded Carboxyl Functionalized Banana Peels."** This work has been carried out by **Pukar Bhattarai** as partial fulfilment for the requirements of an M.Sc. Degree in **Chemistry** under our supervision. To the best of my knowledge, this work has not been submitted for other degree offered in this institution.

.....

Ram Lochan Aryal, Ph.D

Supervisor

Assistant Professor

Amrit Campus, Lainchaur

Tribhuvan University, Kathmandu

Nepal

Tribhuvan University
Amrit Campus
Department of Chemistry

.....

Mr. Naresh Prashad Pant

Co-supervisor

Amrit Campus, Lainchaur

Tribhuvan University, Kathmandu

Nepal

Date Aug-3, 2023

DECLARATION

I, **Pukar Bhattarai,** confirm that the work presented here is genuine work done originally by me and has not been published or submitted elsewhere for any other degree. Any literature, data, or work done by others has been cited in this dissertation work has been acknowledged and are included in the reference section.

.....

Pukar Bhattarai

Date: Aug-3, 2023

ACKNOWLEDGEMENT

This dissertation work is the result of almost a year of effort at the Amrit Campus, Lainchaur. First and foremost, my heartfelt gratitude goes to Asst. Prof. Dr. **Ram Lochan Aryal**, my supervisor, for his real counsel and unwavering support. I am very fortunate to have him as my supervisor. He is a Chemistry legend with huge knowledge and an equally kind and encouraging personality. Mr. **Naresh Prashad Pant**, my co-supervisor, deserves equal credit and thanks for his significant presence, knowledge, and enormous support and guidelines.

I am also thankful to Assoc. Prof. Dr. **Bhusan Shakya,** M.Sc Program Coordinator, for his humility for being a constant source of motivation to students like me committed to research. I am grateful to the Department of Chemistry for providing the chemicals, instruments, and other physical facilities for the execution of this research. I am equally grateful to Assoc. Prof. **Kanchan Sharma,** Head of Department, Chemistry for offering the department's laboratory resources. I am equally grateful to all the professors of the Department of Chemistry for their advice and support. I am grateful to all the lab assistants and other members of the Chemistry Department for their cooperation and moral support.

I am grateful to **Bipeen Dahal**, Jeonbuk National University, Department of BIN Convergence Technology Jeonju, South Korea, for recording the EDX spectra and SEM images of my materials. I am grateful to all of my friends who supported and assisted me throughout this study. Special thanks to Susan Waiba, Surakshya Ghemosu, Bijay Kumar Das, Ganesh Thapa, Arjun Regmi, Manju Regmi and Srijana Bhattarai for help and incredible support. I am thankful to National Youth Council, Sanothimi, Bhaktapur, Ministry of Youth and Sports, **Nepal Government** for financial support. Last but not least, I'd like to thank my family members for the constant support and encouragement during my research study.

"राष्ट्रीय युवा परिषद्को आर्थिक सहयोगमा गरिएको अनुसन्धान"

.....

Pukar Bhattarai

July 2023

LIST OF ABBREVIATIONS

RBP	Raw banana peel
SBP	Saponified banana peel
Fe(III)	Ferric ion
Fe(III)-SBP	Fe(III)-loaded saponified banana peel
mg/g	Milligram per gram
rpm	Rotation per minute
C_i	Initial concentration
C_e	Equilibrium concentration
FTIR	Fourier transformed infrared spectroscopy
EDX	Energy dispersive X-ray
SEM	Scanning electron microscopy
%A	Percentage biosorption
%D	Percentage desorption
k_1	Pseudo-first-order rate constant
k_2	Pseudo-second-order rate constant
q_e	Amount biosorbed at equilibrium
q_t	Amount biosorbed at time
UV-Vis	UV visible spectrophotometer

ABSTRACT

Excessive phosphate in aqueous solution is one of the main factors leading to eutrophication and exploitation of water bodies. It is present as an ingredient in NPK (Nitrogen, Phosphorus, and Potassium) fertilizer. The reserves of phosphate in soil are basically in the form of mineral phosphate and organic phosphate. Demerit of PO_4^{---} and its removal among the available technology, biosorption stands out as the most attractive treatment option. In this work, biosorbents for phosphate ion removal were synthesized from Banana Peel (BP) after saponification followed by Fe(III) loading. The investigated carboxyl functionalized biosorbent biosorbed phosphate ion from aqueous solution through ion exchange and ligand exchange mechanism. The functional group and surface morphology of biosorbents were identified by FTIR and SEM/EDX. The point of zero charge pHpzc was found at pH 6.8. It was found that biosorption capacity depends on the pH, concentrations, contact time, interfering ions and biosorbent doses. The maximum biosorption capacity of Fe(III)-SBP for phosphate was found to be 18.51 mg/g at pH of 5.34. Langmuir isotherm and pseudo second order (PSO) kinetic model well described the experimental data. The increment in concentration of chloride (Cl^-) and nitrate (NO_3^-)showed negligible interference while that of sulphate (SO_4^{--}) and bicarbonates (HCO_3^-) inhibited significantly. The biosorbed phosphate can be effectively desorbed using 0.5M NaOH. The findings showed that Fe(III)-SBP biosorbent investigated in this study seems to be one of the most promising biosorbents for the removal of phosphate ion from aqueous solution.

Keywords: Saponified banana peels, Fe(III)-SBP, Phosphate biosorption, Interfering ions, Aqueous solution

TABLE OF CONTENTS

CHAPTER II

LITERATURE SURVEY/REVIEW, RESEARCH GAPS AND SCOPE OF THE STUDY

CHAPTER III

MATERIALS AND METHODS

LIST OF FIGURES

LIST OF TABLES

Page No.

LIST OF SCHEMES

Page No.

CHAPTER I

INTRODUCTION

1.1 General introduction

Phosphate is necessary for all known forms of life (Dong *et al.,* 2019). It is often present in low concentration in wastewater in the form of phosphate ion (PO_4^{---}), hydrogen phosphate (HPO_4^{--}) and dihydrogen phosphate ($H_2PO_4^{-}$) (Slocombe *et al.,* 2020). Surface run-offs contribute to an extent of 65 % of PO_4^{---} pollution, industrial wastes from detergent manufacturing and fabric treatment add to about 25 % and domestic and municipal sewages accounts to about 10 % (Bijekar *et al.,* 2022). Hence, there is growing awareness towards the PO_4^{---} pollution in the world (Xia *et al.,* 2020). Some countries have made legislation and introduced phosphate control acts, for example Switzerland banned the use of PO_4^{---} in detergent (Shrestha *et al.,* 2018).

It has been estimated that a person contributes to about 2-3 g of PO_4^{---} in wastewater every day (Ruane *et al.,* 2021). Regulatory control on PO_4^{---} disposal is evident all over the world in recent years (Li *et al.,* 2021). Strict regulatory requirements decreased the permissible level of PO_4^{---} concentration (*i.e.* up to 1 mg/L) in wastewater at the point of disposal (Saleh *et al.,* 2021). Hence, it is necessary to find an appropriate solution for treatment of wastewater prior to disposal (Shrestha *et al.,* 2018).

Different protection agencies such as the World Health Organization (WHO) and the US Environmental Protection Agency (USEPA) do not allow the permissible level of PO_4^{---} more than 10 mg/L (Aryal *et al*., 2020). Excess inhalation of PO_4^{---} in human body is detrimental to human health that may cause lethal cardiovascular and cerebrovascular diseases (Rihal *et al.,* 2022). Researchers have been attracted in developing an efficient biosorbent using different biowaste to sequester PO_4^{---} from water (Aryal *et al.,* 2022).

Eutrophication is caused by the excess discharge of phosphate from the municipal or industrial wastes in the sources of water (Preisner *et al.,* 2021). It is increasing in lake, river or other body of water (Ayele *et al.,* 2021). It depletes the level of oxygen which causes reduction in biodiversity (Rommens *et al.,* 2003). It leads to undesirable algal blooms (Clark *et al.,* 1997). Consequently, the removal of phosphate in domestic &

industrial discharges is absolutely necessary to avoid this kind of eutrophication problem (Blaney *et al.*, 2007). When the total phosphate level in the water is between 0.01 and 0.03 mg/L, there is no evidence of algal blooms on the water's surface (Peleka *et al.*, 2009).

The growth in the human population and the rise in the consumption of resources have increased the burden on aquatic ecosystems & have affected the global biogeochemical cycles of carbon (C), nitrogen (N) & phosphorus (P) (O'Boyle *et al.*, 2020). In most cases, phosphate is the limiting factor in the eutrophication process not nitrogen because nitrogen fixation is naturally performed by diazotrophs (Zhang *et al.*, 2022). Therefore, most of the recent nutrient-removal studies have focussed on the removal of phosphate (Lacasa *et al.*, 2011).

Phosphate, on the other hand, is never obtained itself; rather, it always bound to one or more elements in the form of compounds known as phosphates or minerals. It is almost never found in a soluble state (Pasek *et al.*, 2019). It was anticipated that 125 million tons of phosphate rock concentrate and unuseful phosphate rock would be produced across the world for direct processing and direct application, respectively (Cisse, 2004). The following chemical reaction takes place when phosphate is dissolved in water:

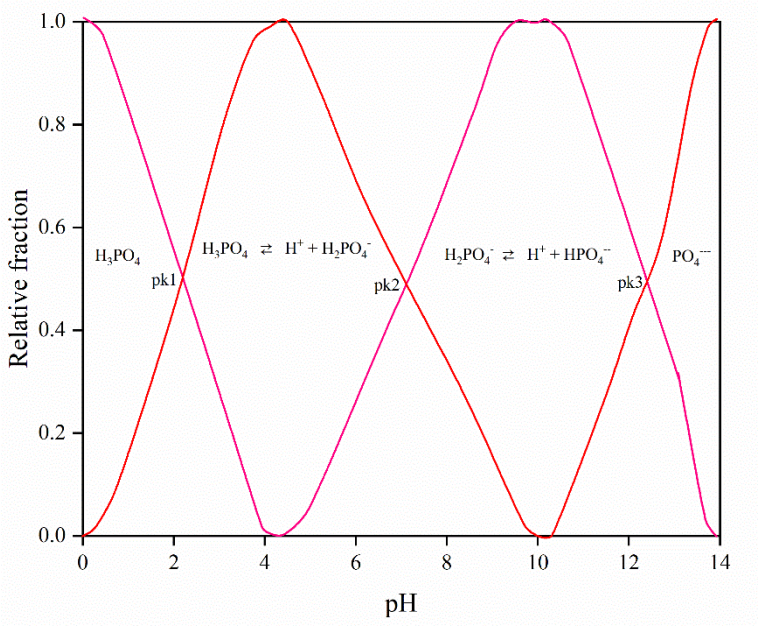

Figure 1.1: Phosphate speciation diagram (Zeitoun *et al.*, 2020)

Fig 1.1 shows that the pH of the aquatic medium controls the speciation of phosphate ion (pk_1 = 2.15, pk_2 = 7.20, pk_3 = 12.33). The orthophosphate ($-PO_4^{---}$) can exist in a variety of ionic species. Since neutral H_3PO_4 has a low affinity for binding sites below pH 2.0, little phosphate is biosorbed from the solution. $H_2PO_4^-$ and HPO_4^{--} are found in the pH range of 2.1 to 7.2. $H_2PO_4^-$ is the main species and is a monovalent species that is significantly biosorbed by ligand exchange interaction. Similar patterns were seen in earlier investigations as well (Biswas *et al.*, 2008). However, at pH values higher than 7.2, there is a considerable concentration of $[OH^-]$ in solution. As a result, repulsion prevents negatively charged HPO_4^{--} species from being biosorbed.

1.2 Different methods for phosphate removal

Some of the traditional ways to remove PO_4^{---} from contaminated water are membrane separation technologies (Hashim *et al.*, 2019), ion exchange (Zhou *et al.*, 2018), chemical oxidation and reduction, precipitation (Liu *et al.*, 2018), co-precipitation (Kondalkar *et al.*, 2019), evaporative recovery (Mishra *et al.*, 2023), electrochemical treatment (Cid *et al.*, 2018), and reverse osmosis (Tripathi *et al.*, 2015). These above methods use a considerable amount of energy, generate hazardous sludge, are costly, and need expensive equipment, and they fail to entirely eliminate phosphate. Chemical treatments are more successful than the other procedures, although they are more expensive (Ahmed *et al.*, 2021). Chemical precipitation is also useful for PO_4^{---} removal, yet it is expensive and less successful when the concentration is low.

Adsorption is found to be a preferable alternative for waste removal since it allows for the effective regeneration and recovery of adsorbed material, which can be reused (Gkika *et al.*, 2022). Biosorption, on the other hand, is recognized as an appropriate technique for PO_4^{---} treatment since it is equally successful for removing both organic and inorganic contaminants.

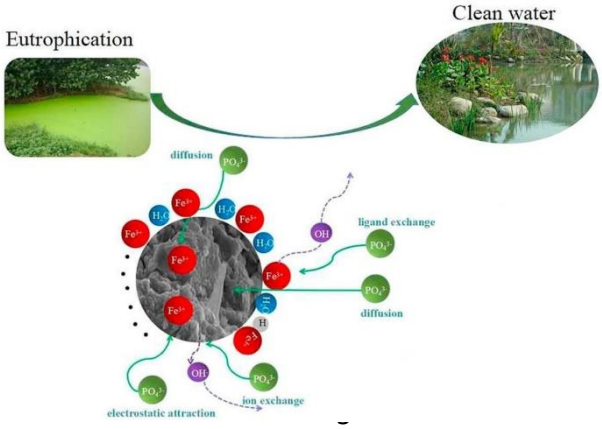

Figure 1.2: Mechanism of phosphate biosorption (Vikrant *et al.,* 2018)

Fig. 1.2 shows the pond with algal blooms, clean water pond and the mechanism of biosorption of PO_4^{---} by ion exchange, ligand exchange and electrostatic attraction. Ligand exchange and ion exchange occurs by the replacement of OH^- by PO_4^{---} and electrostatic attraction occurs between Fe(III) and PO_4^{---}.

1.3 Low-cost biosorbents for phosphate removal

As reported in literature, many types of agricultural waste have been used in PO_4^{---} removal process. There is a growing interest among researchers in using agro-waste products to remove contaminants present in polluted water (Ashokkumar *et al.,* 2021). The main issue in this process is to identify an entirely efficient biosorbent that can be made from readily available materials (Yaashikaa *et al.,* 2021).

Sugarcane bagasse (Carvalho *et al.,* 2011), peanut shell (Jung *et al.,* 2015), apple pomace (Thangavelu *et al.,* 2022), sawdust (Lou *et al.,* 2016), coconut husk (Thongsamer *et al.,* 2022), orange peel (Chen *et al.,* 2022), litchi seed waste (Piol *et al.,* 2021), pine bark (Xu, 2009), coir pith (Kumar *et al.,* 2010), and juniper bark (Shin *et al.,* 2007). Chemical modifications of hydroxyl group-rich biosorbents including cellulose, hemicellulose, pectin and lignin have been used to enhance a wide range of chemical reactions and influence biosorbent properties. Loading of higher valent metals into biomaterials produces positively charged metal ions along with hydroxyl ligands that are good for binding negatively charged anions like phosphate (PO_4^{3-}).

1.4 Banana peel as biosorbent and its chemical significance

Banana is one of the most significant crops in the world, and it is cultivated in more than 130 different nations (Kumar *et al.,* 2018). According to Ali *et al.,* (2016), the top 10 banana-producing countries in the world are as follows: India, China, Uganda, the Philippines, Ecuador, Brazil, Indonesia, Colombia, Cameroon, and Ghana. In a country similar to ours, bananas are either grown domestically or imported in large quantities (Schnurr *et al.,* 2020). Peels of bananas is a cellulosic biomass that has the potential to be changed to increase the number of binding functional sites that are suitable for biosorption (Akpomie *et al.,* 2020). There are a variety of low molecular weight species present in banana peels, including cellulose (7.6–9.6%), hemicellulose (6.4–9.4%), pectin (10–21%), and proteins (10.2-12.1%) (Emaga *et al.,* 2008). The presence of methyl ester groups of pectin is responsible for chemical modification

(Wang *et al.,* 2019). Pectin has a carboxy group, which makes it easy to convert into functionalized biosorbent obtained through the saponification process (Arya *et al.,* 2022). Saponification is the process for the transformation of methyl ester groups to carboxyl group structures (Hu *et al.,* 2018). To the best of my knowledge, banana peel powder loaded with Fe(III) has not been synthesized for phosphate (PO_4^{3-}) removal so far.

When rare metals are loaded into biomaterial, ligand exchanger are produced with positively charge metal in center. These positively charged metal ions are ideal for the retention of negatively charged anions such as phosphate (Zhang *et al.,* 2021). Hence, metal loading into biosorbents is the method of choice since it is effective, and it increases affinity for the PO_4^{---} ion biosorption (Nguyen *et al.,* 2014). Mechanisms of phosphate biosorption onto Fe(III) loaded biosorbents include electrostatic attraction, ligand exchange mechanism or ion exchange method (Zhang *et al.,* 2011).

Exploration of Fe(III)-loaded carboxyl functionalized banana peel and investigation of biosorption of phosphate anion present in aqueous solution. To the best of my knowledge, Fe(III)-loaded banana powder is a new material that is not studied yet for PO_4^{---} bisorption from aqueous solution. This will be beneficial for our society and nation and it also meets SDG, Goal 6 (THE 17 GOALS, UN).

1.5 Factors affecting biosorption

In batch experiments, the process of biosorption is influenced by a number of factors, including pH, the initial concentration of sorbate, the mass of a biosorbent, time interval that sorbate and biosorbent are in contact with one another, the presence of other anions (Thirunavukkarasu *et al.,* 2021). The biosorption process can be evaluated with alterated parameters.

1.5.1 Effect of pH: The pH of the solution is significant because it influences both the behaviour of the external functional groups of the biosorbent and the aqueous chemistry of the sorbate ions (Vijayaraghavan *et al.,* 2008). PO_4^{---} are significantly affected in terms of their speciation and their availability for biosorption. There is a correlation between a rise in the pH and an increase in the number of negatively charged surface groups. This leads to an increase in the biosorption capacity. This results in an improvement in biosorption. On the other hand, a lower pH enhances the

capacity to be biosorbed since there are more positively charged surface functional groups present in the biosorbent (Aryal *et al.*, 2010).

1.5.2 Effect of dose: The quantity of biosorbent used for the biosorption is known as dose effect. The dosage of the biosorbent has a significant impact on biosorption. On increasing the amount of biosorbent, the % biosorption is calculated (Aryal *et al.*, 2011). When the amount of biosorbent is increased, the process of biosorption goes up. This can be attributed to the increase in the number of binding sites (Tangaromusk *et al.*, 2002).

1.5.3 Effect of contact time: On long exposure of biosorbent with sorbates, a greater number of surface binding sites will be exposed, which will encourage biosorption (Vijayaraghvan *et al.*, 2008). There will be more chances of biosorption of an anion with the sorbates.

1.5.4 Effect of initial concentration: The biosorption capacity increases with increase in the initial concentration. It is because the number of PO_4^{---} anions are relatively higher at higher concentrations (Sherlala *et al.*, 2018). The interactions between the sorbates and biosorbent increases as the concentration does due to the increase of concentration gradient.

1.5.5 Effect of competing ions: The presence of a variety of competing ions may have an effect on the biosorption capacity of the biosorbent. Existence of co-ions in water has the potential to induce interference as well as competition for biosorption sites. It is possible to have a comprehensive understanding of the influence of co-ions or competing ions in order to maximize the biosorption of PO_4^{---} anions (Aryal *et al.*, 2011). A wide variety of ions are found in water that has been contaminated by pollution. The presence of competitive ions can either enhance or decrease the biosorption capacity of biomass (Saravanan *et al.*, 2022).

1.6 Biosorption studies

A surface phenomenon known as biosorption is the process by which chemical components that are in the fluid phase become attached to the surface of a liquid or solid (Salam *et al.*, 2019). The term "biosorbent" refers to the solid substance that offers a surface for biosorption, while "sorbate" refers to the species that are

biosorbed by the biosorbent. It can take place either physically (which is referred to as physisorption) or chemically (which is referred to as chemisorption). In physiosorption, a weak Vander Waal's force is involved between the sorbate and the biosorbent, whereas in chemi-sorption, molecules bind to the surface by creating strong chemical bonds. Physisorption is a subset of chemisorption (covalent bonds, hydrogen bonds).

The following formula may be used to get the percentage of biosorption (in %) and the quantity of sorbate biosorbed in mg/g when the system is at equilibrium:

$$\% \text{ A} = \frac{C_i - C_e}{C_i} \times 100\% \qquad \textbf{(1)}$$

$$q = \frac{C_i - C_e}{W} \times V \qquad \textbf{(2)}$$

where C_i and C_e represent the initial and equilibrium concentrations of solution in mg/L respectively. In the experiment, V represents the amount of phosphate solution that is used (in litres), and W represents the amount of the biosorbent that is used (in grams).

1.7 Kinetics studies

It gives specific information about how biosorption works in the batch process. This process focuses on getting rid of the pollutant in two stages: first, quickly, and then slowly, until equilibrium is reached. How well the biosorption process works depends on how quickly sorbates are taken up by biosorbents. This rate also influences the kinetics of the biosorption process (Aktar *et al.*, 2021). Pseudo-first-order and pseudo-second-order models are two models of those that may be used to represent the interactions that take place between the biosorbent and the particles that are biosorbed (Ho *et al.*, 1998). The accuracy of any model may be measured by the determination of coefficient (R^2), which should be close to 1 if the model accurately represents the kinetics of the biosorption process. These two models are used in virtually for all biosorption processes.

1.7.1 Pseudo-first-order (PFO) model

The PFO kinetic model was first proposed by Langragen in 1898 (Huang *et al.*, 2022). It is based on the idea that the rate of biosorption is directly related to the number of empty sites. The equation for the rate is as follows:

$$\frac{dq_t}{dt} = k_1(q_e - q_t) \qquad \textbf{(3)}$$

where k_1 is the PFO rate constant, q_e and q_t are the amounts of sorbate per unit mass of biosorbent at the equilibrium time (t), and t is the time interval (min^{-1}). After integration and application of the boundary conditions t = 0 to t = t, and similarly, q_t = 0 to q = q_t, the linearized form of the equation is as follows:

$$\log (q_e - q_t) = \log q_e - k_1 t \qquad \textbf{(4)}$$

A straight line is obtained when log (q_e – q_t) is plotted against time; from this line, k_1 and q_e may be calculated by making use of the slope and the intercept of the plot, respectively. It is possible to rewrite **equation (4)** in a form that is in non-linear form as

$$q_t = q_e(1 - e^{-k1t}) \qquad \textbf{(5)}$$

1.7.2 Pseudo-second-order (PSO) model

According to the Ho and Mckay equation, which is followed by the PSO kinetic model, chemisorption operates as a rate-limiting phase and incorporates valence forces through the exchange of electrons between the biosorbent and the sorbate. In this concept, the chemisorption process is the one that slows down with time, and the capacity of the biosorbent is directly proportional to the number of active sites present on the biosorbent. (Ho *et al.*, 1998) In its general version, the equation for the PSO rate is expressed as follows:

$$\frac{dq_t}{dt} = k_2(q_e - q_t)^2 \qquad \textbf{(6)}$$

where k_2 is the second-order rate constant of biosorption expressed as (g/mg min). The amount of the sorbate that has been biosorbed at equilibrium is denoted by the symbol q_e (mg/g), and the amount of the sorbate at time t is denoted by q_t (min), integrating equation for boundary conditions: from t = 0 to t = t and, accordingly, from q_t = 0 to q_t = q_t; the integrated version of the equation is as follows:

In its linear form, **equation 6** may be rearranged as follows:

$$\frac{t}{q_t} = \frac{1}{k_2 q_e^2} + \frac{1}{q_e} \text{t} \qquad \textbf{(7)}$$

where k_t represents the first-order reaction rate constant for biosorption (min^{-1}). The values of k_1 and q_e may be derived from the slope and the intercept of the plot of $\log(q_e - q_t)$ *versus* t, respectively. On the other hand, the values of k_2 and q_e are similar when derived from the intercept and the slope of the plot of t/q_t *versus* t (Mekonnen *et al.,* 2015).

1.8 Isotherms studies

An isotherm is a graphical depiction of the quantity of sorbate per unit mass of biosorbent as a function of the concentration of sorbate that is still present in the solution when it has reached equilibrium at a constant temperature and pH (Sahu *et al.,* 2021). An isotherm study can be helpful in evaluating how biosorbent interacts with sorbate, revealing the biosorption capability of biosorbent, and gaining knowledge how biosorption works as a mechanism. Both the Langmuir and the Freundlich isotherm models are utilized often in the process of biosorption process.

1.8.1 Langmuir isotherm model

The Langmuir isotherm is based on the idea that biosorption occurs as a single layer on uniform surfaces (Priyadarshanee *et al.,* 2021). There is no interaction between the molecule that is being adsorbed and the site that is next to it since each active site can only capture a single molecule of sorbate. As a result, the biosorbent has a limited capacity once it reaches the saturation point, and no further biosorption processes can take place.

$$q_e = \frac{q_m . b . C_e}{1 + \text{b}.C_e} \qquad \textbf{(8)}$$

where, C_e is the equilibrium concentration of sorbate (mg/L), q_e is the amount of phosphate biosorbed at equilibrium (mg/g), q_m is the maximum amount of biosorption that can occur with complete monolayer coverage on the biosorbent surface (mg/g), and b is the Langmuir constant (L/g), which is related to the amount of energy for biosorption reaction (Langmuir, 1918). It is possible to linearize the Langmuir equation using the following form:

$$\frac{C_e}{q_e} = \frac{1}{q_m.b} + \frac{C_e}{q_m} \qquad \textbf{(9)}$$

The slope and intercept of the Langmuir plot of Ce/q_e *versus* C_e can be used as a basis for computing the values of q_m and b, respectively. The equilibrium biosorption process may be better understood with the help of the information provided by the Langmuir parameters q_m and b.

1.8.2 Freundlich isotherm model

The Freundlich isotherm mainly describes the biosorption equilibrium of multiphase biosorption surfaces owing to the sorption enthalpy assumed to be unevenly distributed on the surface of the biosorbent with an increase in surface coverage (Wang *et al.,* 2016). Freundlich's empirical equation for biosorption (Freundlich, 1906) is as,

$$q_e = K_f \,.\, (C_e)^{1/n} \qquad \textbf{(10)}$$

where K_f is the Freundlich isotherm constant expressed in (mg/g), n equals the amount of biosorption and C_e is the sorbate concentration at equilibrium, measured in (mg/L). q_e is the amount of sorbate (mg/g) that can be taken up by one gram of the biosorbent at equilibrium. The following equation serves as a linearized representation of the Freundlich isotherm:

$$\log q_e = \log K_F + \left(\frac{1}{n}\right) \log C_e \qquad \textbf{(11)}$$

Where K_F and n are the Freundlich constants for the biosorption capacity and intensity, respectively. There is a significant affinity between phosphate ions and surface binding sites if the Freundlich constants (K_F) and 1/n, have high values. On the other hand, the heterogeneity factor has a lower value for more heterogeneous surfaces since it has a lower value for the Freundlich constants. The constants K_F and 1/n may be computed by using the intercept and slope of the straight line that results from plotting $\log(q_e)$ *versus* $\log(C_e)$. This plot reveals a linear relationship between the two variables (Moyo *et al.,* 2013). If n is equal to 1, then the partition between the two phases is unaffected by the concentration of the substance (Riederer *et al.,* 1990). All surface locations are equal. The value of 1/n has direct relation on the efficiency of the biosorption process. If 1/n is less than 1, indicates typical biosorption is occurring, and if it is greater than 1, suggests that cooperative biosorption is occurring.

1.9 Different methods for determination of phosphate concentration

There are a few different approaches that may be used in order to calculate the amount of phosphate that is present in the liquid medium (Krishnaprabu *et al.,* 2020). Measurements that are both very sensitive and analytical are necessary in order to ascertain whether or not PO_4^{---} is present in the soil or the water. For the determination of PO_4^{---} at higher concentrations, analytical methods such as titrimetric and complex-gravimetry have been proposed. However, at mg/L levels, PO_4^{---} can be detected using colorimetry, atomic adsorption spectroscopy, flow injection analysis, high-performance liquid chromatography (HPLC), ion chromatography (IC), inductively coupled plasma atomic emission spectroscopy (ICP-AES) and other similar techniques (Ganesh *et al.,* 2012). Although there are various ways available for determining the presence of PO_4^{---} at trace levels, it is not possible to use all of these methods in typical laboratories due to factors such as the cost, the handling of the necessary equipment, the requirement for an extraction procedure, etc.

1.10 Spectrophotometric determination

The most common way to figure out how much inorganic phosphate used as a reducing agent to turn phosphomolybdate complex into molybdenum blue (MB) in acidic conditions and then use spectrophotometry (Worsfold *et al.,* 2015). This method is based on the reduction of the phosphomolybdate complex into molybdenum blue (Carvalho *et al.,* 1998). The process begins with the synthesis of polyoxometalate species (heteropoly acids) from orthophosphate and molybdate under acidic circumstances (McKelvie *et al.,* 2015). This heteropoly acid is then reduced with an appropriate reducing agent to generate a vividly blue-coloured Phosphomolybdenum complex ion $[H_4PMo(VI)_8Mo(V)_4O_{40}]^{3-}$ (Nagul *et al.,* 2015). The reaction that produces molybdenum blue is carried out in two stages: i) the formation of the Kegging ion surrounding the analyte ii) the reduction of this heteropoly acid to the deep blue complex.

All MB techniques need a strong acid, a source of molybdenum Mo(VI), and a reductant to make the complex. The concentrations of acid and molybdate are important for making heteropoly acid and controlling how it is reduced (Kolev *et al.,* 2015). The following reaction is what happens during the process that leads to the

creation of molybdenum blue:

$$PO_4^{3-} + 12(NH_4)_2MoO_4 + 27H^+ \longrightarrow (NH_4)_3PO_4.12MoO_3 + 21NH_4^+ + 12H_2O$$

$$(NH_4)_3PO_4.12MoO_3 + \text{reducing agent} \longrightarrow [H_4PMo(VI)_8Mo(V)_4O_{40}]^{3-}$$

Phosphomolybdenum blue complex

Using an ultraviolet-visible spectrophotometer, a determination of the newly formed complex is made spectrophotometrically (Duan *et al.,* 2020). Because of its high precision, high detection efficiency, non-destructive sampling, environmentally friendly and low cost. UV-Visible technology has been utilized as an effective tool for assessing the presence of contaminants in water settings (Guo *et al.,* 2020). The Beer-Lambert law serves as the foundation for the operation of this UV-visible spectrophotometer, which measures the amount of ultraviolet or visible radiation that is absorbed by a substance (Ye *et al.,* 2020). When a beam of monochromatic parallel light is directed at the surface of a medium with a specific thickness, the medium absorbs some of the light energy, which results in a decrease in the intensity of the light that is transmitted through the medium (Liu *et al.,* 2020). Beer and Lambert law states that the amount of light that is absorbed by a medium is directly proportional to the thickness of the medium.

$$A = \varepsilon bc \qquad \textbf{(12)}$$

'A' stands for the absorbance of the solution, ε for the molar extinction coefficient, b for the path length, and c for the concentration. The difference in concentration is directly related to the absorbance, and this is true for different solutions with the same wavelength and path length. Hence, concentration can be determined through the measurement of absorbance.

1.11 Statement of problem and its possible solution

The phosphate contamination in the groundwater and surface water is an alarming issue that is causing eutrophication in lakes and rivers, a reduction in dissolved oxygen, and toxicity to aquatic life. Exposure of phosphates lead to uncontrolled growth of algae, which causes the reduced water oxygen content and production of toxins particularly in shallow lakes, coastal marine regions, leading to fish kills with

an elevated risk of skin, bladder, and kidney diseases. Usually used as insecticides, herbicides, or wood preservatives because of their germicidal qualities and resistance to rotting and decay. Phosphates and its parts can move about in the environment and cannot get rid of. However, when phosphates interact with oxygen or other molecules found in the air, water, or soil, as well as with bacteria that live in soil or sediment, it can change its shape, attach to other particles, or detach from these particles and cause eutrophication. Many common phosphorus compounds may dissolve in water, phosphate can pollute lakes, rivers, and subterranean water. It can accomplish this by dissolving in precipitation, ice, or discarded industrial waste. Globally phosphate contamination in wastewater posses a serious concern to human health and ecosystem. Therefore, the target of the present study is to provide cost-effective technology for the removal of phosphate from aqueous solution.

1.11.1 Banana peel

Galacturonic acid groups in pectic components of polysaccharides have been demonstrated to be efficient on removing cationic pollutants, which contributes to the ion exchange properties of polysaccharides. Pectic and lignocellulosic materials are typically saponified with $Ca(OH)_2$ treatment, which enhances their properties such as water retention and swelling, boosts their cation binding/exchange capacity. The cation exchange capacity of banana peels was enhanced with the increment of carboxyl groups into the biopolymer matrices. In addition, for the removal of phosphates from aqueous solution, banana peel powder can be modified as an anion exchanger *via* loading Fe(III) ions after $Ca(OH)_2$ treatments. This study is a novel work since it makes use of chemically modified banana peels for the biosorption of PO_4^{3-}. To the date, no studies have been conducted on the use of Fe(III)-SBP as an anion exchanger for removing oxyanions of phosphorous.

1.12 Objective of the study

1.12.1 General Objective

Exploration of Fe(III)-loaded carboxyl functionalized banana peel and investigation of biosorption of phosphate anion present in aqueous solution.

1.12.2 Specific Objective

- Development of the anion exchanger of Fe(III)-loaded carboxyl functionalized banana peel and investigate its biosorption performance under batch mode.
- Characterization of biosorbents using the characterizing tools like FTIR, SEM/EDX.
- Computation of kinetics and isotherm studies of biosorption process.

CHAPTER II

LITERATURE SURVEY/REVIEW, RESEARCH GAPS AND SCOPE OF THE STUDY

2.1 Literature survey/review

A survey revealed that numerous studies have been carried out around the globe to remove phosphate from water. Biosorption method has been demonstrated to be one which is not only cost-effective but also convenient and eco-friendly to the environment. The biosorption of phosphate through chemically modified agricultural wastes has recently emerged as a potential alternative because it is both promising and environmentally beneficial.

According to Clark *et al*., (1997), the three most important salts for phosphate elimination are calcium, aluminium, and iron. The average phosphate elimination efficiency with chemical dosing using iron(II) was 85.3%. The chemical weight ratio (1:1.50) (P:Fe) resulted in the most effective phosphate removal efficiency, whereas the weight ratio of 1:1.14 (P:Fe) resulted in the least efficient removal after dosing. The iron dose was calculated using an effluent phosphate content of 8 mg/L. Dosage ratio of 2.80:1 (Al:P) was required for phosphate removal in aerated lagoons. For an average effluent concentration of 4.80 mg/L, this dosage reduced phosphate by 90%.

Ye *et al*., (2006) studied the pH effect on PO_4^{---} adsorption for acid thermally treated palygorskite, ranging from 7.80 mg P/g at pH 4.2 to 5.70 mg P/g at pH 8.9. PO_4^{---} adsorption kinetic tests at 25°C revealed that the bulk of PO_4^{---} adsorption on the adsorbents was accomplished in 1-2 hours. The PO_4^{---} adsorbed on the modified acid and thermally treated palygorskite after 2 hours was 90%. When the PO_4^{---} equilibrium concentration increased from 0 to 100 mg P/L, so did the PO_4^{---} adsorption capacity. At a PO_4^{---} equilibrium concentration of 100 mg/L and pH 7.0-7.2, the capacity of acid and thermally treated palygorskite was around 9 mg P/g adsorbents.

Blaney *et al.,* (2007) studied PO_4^{---} sorption is the greatest in the pH range of 6.0-8.0. In less than ten bed volumes, a single step alkaline brine regeneration reliably recovered more than 90% PO_4^{---}. HAIX was used in numerous PO_4^{---} removal cycles.

For more than two years, the identical HAIX particles (spherical beads) were utilized in batch testing and column runs without physical degradation. PO_4^{---} isotherms at three distinct temperatures, 7, 23, and 37°C, under similar experimental circumstances revealed that temperature had no effect on PO_4^{---} absorption.

Kumar *et al*., (2007) showed that pLEs can successfully remove more than 85% of the adsorbed PO_4^{---} from exhausted medium and precipitate as $MgNH_4PO_4.6H_2O$. The optimal molar ratio for precipitating struvite from RO concentrate was determined to be Mg^{2+}:NH_4^+:P::1.5:1:1 at pH 9.0.

Riahi *et al*., (2009) analysed the PO_4^{---} adsorption capacity (4.35 mg/g) was observed at pH 6.8 for an adsorbent dose of 6 g/L, an initial PO_4^{---} concentration of 50 mg/L, and at constant temperature of 180° C ± 02, with the equilibrium state attained within 120 minutes of exposure time.

The Al industry generates a huge amount of red mud waste. The results demonstrated that the produced coagulant could decrease PO_4^{---} levels to less than 0.02 mg/L. It increased PO_4^{---} removal efficiency from 4.9% to 10.4% as compared to commercial polyaluminium chloride coagulant (PACI). The optimum coagulation performance occurs at pH value 6. The experimental findings revealed that the PO_4^{---} removal efficiency rose significantly with reaction time (from 1h to 4h), then gradually increased after the reaction period beyond 4h. It is clear that the PO_4^{---} removal effectiveness declined gradually as the temperature of the aqueous solution lowered (Zhao *et al*., 2011).

During the electrocoagulation studies using Fe and Al electrodes, the content of phosphates in the aqueous solution was reduced to less than 0.1 mg dm^{-3}. The current density was a crucial element in the PO_4^{---} removal process, particularly when iron electrodes were utilized, as efficiency increased at lower current densities. Al and PO_4^{---}, as well as $Al(OH)_3$, competed in the pH range utilized, however the synthesis of Al_3PO_4 was aided by the low current densities (Lacasa *et al*., 2011).

Sun *et al*., (2013) conducted an experiment that lasted around 430 days. For municipal wastewater, the whole treatment time is less than 10 hours. At effluent concentrations of less than 1 mg/L, an MBR-based procedure removed 27% of total PO_4^{3-}.

Nguyen *et al*., (2013) investigated okra was cationized with $FeCl_3$ 0.25M (iron loaded okra, ILO) to improve its PO_4^{---} adsorption ability. PO_4^{3-} sorption onto ILO was successful at pH 3 conditions, with a starting PO_4^{---} content of 25 mg/L, a biosorbent dosage of 20 mg/L, and a contact period of 7 hours. According to the Langmuir model, the maximal PO_4^{---} adsorption capacity of ILO was 4.785 mg/g. The PO_4^{---} removal effectiveness was greater than 90%.

At 25°C, the highest biosorption of *K. alverezii* was 59.77 mg/g and matched the Redlich-Peterson model. The biosorption of *K. alverzii* increased with temperature and was greatest at pH 6.0. The surface of *K. alverezii* becomes PO_4^{---} saturated at a bio-sorbent dosage of 3.0 g/L. Chemisorption was often described using the PSO kinetic model (Rathod *et al*., 2014).

According to Wang *et al*., (2015), LH pine needles were efficient throughout a wide pH range, with the best removal effectiveness occurring at a pH of 3. The initial PO_4^{---} content of 5 mg/L produced the maximum removal efficiency. In the trials that followed, 720 minutes was determined to be the ideal duration. The PSO kinetic model fits better with the sorption process. The Langmuir model had an excellent match to the data (R^2>0.97).

For the elimination of PO_4^{---}, the highest adsorption capabilities were determined to be 96.5 mg/g and 100 mg/g, respectively. It was discovered that pH 3 is the ideal pH for PO_4^{---} adsorption. It was discovered that the equilibrium contact period for the sorption of PO_4^{---} was 240 minutes. PO_4^{---} was best taken in at a dosage of 17 mg. The maximal adsorption capabilities for PO_4^{---} were determined to be 100 mg/g by FeCLW and 96.5 mg/g by FeRLW (Shrestha *et al*., 2018).

Bouamra *et al*., (2018) demonstrated that the linear Langmuir model suited the sorption of PO_4^{--} onto PWM (powdered marble) well. PSO kinetic model governs the adsorption process. The PO_4^{---} removal increased from 34.7 to 97.8%, raising the final pH from 6.81 to 8.44. The effectiveness of PO_4^{---} removal was around 94.5% between 50 and 100 rpm at the period of 60 min. At an adsorption temperature of 40°C, PO_4^{---} removal was shown to be about 93.6%.

The UF MMR was created by combining amorphous powder with polymer ($C_2H_2F_2$). NO_3^- and PO_4^{3-} had MMR adsorption capacities of 9.66 mg-N/g and 15.58 mg-P/g,

respectively. Adsorption was governed by a PSO kinetic model. The UF MMR has a high permeability (500 LM/MPa). UF membranes combining polysulfone (PSf) and polyvinylpyrrolidone (PVP) have a good PO_4^{---} removal efficiency (93.6%) but a low permeability of 48 (MH/MPa) (Gao *et al*., 2019).

Qu *et al*., (2020) studies revealed that the La-Fe-BC, exhibited an excellent monolayer PO_4^{---} uptake of 330.86 mg/g over a wide pH range of 3.0-8.0, separation efficiency of 91%. As observed, the co-existence of Cl^- had a negligible effect on PO_4^{---} adsorption with above 98%. It followed PSO kinetic model and Langmuir models.

In batch experiments, the BR-N could efficiently remove PO_4^{---} over a wide pH range of 5.0 to 9.0, and its highest PO_4^{---} adsorption capabilities were 34.40 mg P/g. BR-N continued to show >82% adsorption capacity for phosphate removal after 8 continuous cycles of adsorption-desorption. The PO_4^{---} equilibrium pH is 7.0 with a qe of 13.73 mg P/g. Within 100 minutes, the adsorption equilibrium was reached. The data may be well represented by the PSO kinetic model (R^2 = 0.993). Langmuir's model was best fit for the isotherm data (Pan *et al*., 2020).

The Freundlich isotherm model accurately explained phosphate adsorption on BC-N (biochar generated with N_2), although the Redlich-Peterson model best suited the data. The maximal adsorption capacities for BC-N, BC-C, FBC-N, and FBC-C, respectively, were 9.63, 8.56, 16.43, and 19.24 mg Pg^{-1}, showing higher adsorption by Fe(III) loaded chitosan-biochar composite fibres (FBCs). The PFO kinetic model adequately explained phosphate adsorption on BC-C and BC-N, but FBC-N and FBC-C data were explained by the PSO and Elovich models, respectively. At pH 2, FBCs had the maximum PO_4^{---} removal effectiveness. Nevertheless, at pH 4, significant PO_4^{---} removal efficiency was reported. The optimal conditions for maximum PO_4^{---} removal were solution pH 4.0 and adsorbent dose 2 gL^{-1} (Palansooriya *et al*., 2021).

Sodium hydroxide (NaOH) saponification and $FeCl_3$ cationization were used to activate pomegranate peel (PP) ($FeCl_3$). At pH 9 and 25°C, a successful elimination of PO_4^{---} up to 90% was accomplished in 60 minutes with the help of 150 mg of Fe-rich pomegranate peel. The findings demonstrated that the Elovich model, which posits that the chemisorption process (PSO) predominates, provides the best match for the kinetics (R^2=0.97), but the isotherm obeys both the Langmuir (R^2=0.98) and

Freundlich (R^2 =0.94) models, with a maximum PO_4^{---} uptake of 49.12 mgg^{-1} (Bellahsen *et al*., 2021).

At a pH of 4.0, it was discovered that the maximal biosorption capacity for PO_4^{---} was 27.63 mg/g. Interfering ions don't have a noticeable impact. The examined biosorbent's point of zero charges (pH_{pzc}) was discovered to be 5.6. The Langmuir isotherm model can provide a more comprehensive explanation for the isotherm investigations in the biosorption of PO_4^{---} onto Zr(IV)-SWR. A PSO kinetic model successfully explained the experimental results, according to kinetic studies. With a NaOH concentration of 0.3M, the maximal desorption of PO_4^{3-} was discovered to be 99.65% (Aryal *et al*., 2022).

The adsorbent's maximum PO_4^{---} removal rate exceeded 97%. relatively wide pH range (3.7-10.8). According to calculations made with the Langmuir model, the maximal adsorption capacities of Ni-La@Peel were 226.55 mg P/g and 220.31 mg P/g under alkaline and acidic conditions, respectively. All of the findings, however, were in agreement with the Langmuir isothermal (R^2=0.99), demonstrating that homogenous chemisorption (PSO) was primarily responsible for the PO_4^{---} removal process of Ni-La@Peel. According to experimental findings, PO_4^{---} ability to bind to other anions such Cl^-, SO_4^{--}, NO_3^-, Br^-, and F^- only decreased by roughly 10% when compared to the blank sample. Also, at the seventh adsorption-desorption cycle, Ni-PO_4^{---} La@Peel's removal efficiency was at 82.05% (Akram *et al*., 2022).

2.2 Research gaps and scope of the study

The reported studies revealed that zeolites, activated carbons, synthetic chelating resins etc. were utilized for the efficient removal of PO_4^{---} from aqueous solution. However, these materials are expensive, low selectivity and produces secondary toxic sludge etc**.** Researchers have long been interested in the possibility of developing adsorbent, that is low in cost, safe for the environment, and, most importantly, has the ability to remove even a trace quantity of phosphate ions from water. In order to address it, agricultural bio-wastes were chemically modified to form efficient biosorbents. In the past, various wastes from citrus fruits have been used for the removal of PO_4^{---}, but research related to banana peel by loading Fe(III) after saponification has not been done yet. Peel from *Musa paradisiaca* (banana), which is not only readily available but also abundant in quantity, can be utilized for the efficient removal of PO_4^{---} from an aqueous solution.

CHAPTER III

MATERIALS AND METHODS

3.1 Instruments

The instruments used during the research work are listed below:

Table 3.1: List of instrument names, their model number and manufacturer

Instrument name	Model number	Manufacturer	Manufacturing Country
Laboratory mill (grinder)	LM-05	Chinetti	Italy
Sieve number 150 μm	E11	Retsch	Germany
Weighing balance model	ASN-224	Phoenix instrument	Germany
Magnetic stirrer hot plate	L34	Labinco	Netherlands
Shaker	SF1	Stuart Scientific	United Kingdom
Digital pH meter	LT-11	Labtronics	India
Spectrophotometer	LT-2802	Labtronics	India
FTIR	10.6.2	PerkinElmer	New Zealand
Oven	UN30	Elite Oven	United Kingdom

3.2 Chemical reagent

All the chemicals used were of laboratory/analytical grades, which are listed below in table.

Table 3.2. List of chemicals used throughout the dissertation work

S.N	Name of Chemicals	Manufacturer Name	% Purity
1	Ammonium heptamolybdate $[(NH_4)_6MO_7O_{24}.4H_2O]$	Qualigens fine chemicals	98
2	Buffer tablets of pH 4.7 and 9.2	Qualigens fine chemicals	96
3	Calcium hydroxide ($Ca(OH)_2$)	E. merck	96
4	Hydrochloric acid (HCl)	Qualigens fine chemicals	97
5	Potassium antimony (III) oxide tartrate hemihydrate $[K_2(SbO)_2C_8H_4O_{10}.3H_2O]$	Merck life	99
6	Oxalic acid ($C_2H_2O_4$)	Qualigens fine chemicals	99.5
7	Sodium dihydrogen orthophosphate (NaH_2PO_4)	E. merck limited	98
8	Sodium bicarbonate ($NaHCO_3$)	Qualigens fine	99.9

		chemicals	
9	Sodium carbonate (Na_2CO_3)	Qualigens fine chemicals	98
10	Sodium chloride (NaCl)	Thermo fischer scientific	99.5
11	Sodium hydroxide (NaOH)	Fischer scientific	98
12	Sulphuric acid (H_2SO_4)	Qualigens fine chemicals	98
13	Fe(III) chloride ($FeCl_3$)	Loba chime pvt. Ltd.	64.5-70
14	Ascorbic acid ($C_6H_8O_6$)	Roche	90

3.3 Preparation of reagents

3.3.1 Preparation of 1000 mg/L stock phosphate solution

Accurately weighed 1.64g of ($NaH_2PO_4.2H_2O$, 156.01) was dissolved in a few ml of distilled water. It was produced to 1000 mL volumetric flask and fill upto mark with distilled water after thoroughly shaking.

3.3.2 Preparation of ammonium molybdate reagents:

3.3.2.1 Ammonium molybdate reagent (I)

12g of $(NH_4)_6MO_7O_{24}$ was dissolved in 87.5 mL of distilled water. The solution was then allowed to cool after 140 mL of concentrated H_2SO_4 was added to 200 mL of distilled water. This cooled content was mixed with $(NH_4)_6MO_7O_{24}$ solution and diluted to the mark in the 500 mL volumetric flask which is termed as ammonium molybdate reagent (I).

3.3.2.2 Ammonium molybdate reagent (II)

20g of $(NH_4)_6MO_7O_{24}.4H_2O$ was dissolved in 250 mL of distilled water in a 500 mL V.F. The 500 mL V.F was then progressively filled with 198 mL of reagent (I) and allowed to cool. The mixture was diluted to 500 mL V.F to get a 0.5% (w/v) solution.

3.3.3 Preparation of $K_2(SbO)_2C_8H_4O_{10}.3H_2O$

0.02g of $K_2(SbO)_2C_8H_4O_{10}.3H_2O$ was dissolved in 100 mL distilled water for every experiment.

3.3.4 Preparation of 5N H_2SO_4 solution

In a 500 mL V.F., 68.8 mL of concentrated H_2SO_4 (98%) solution was diluted with distilled water to make 5N H_2SO_4 solution.

3.3.5 Preparation of 0.1N HCl solution

In a 500 mL volumetric flask, 4.5 mL of concentrated HCl solution was added into water, and the volume was added to obtain 0.1 M HCl solution.

3.3.6 Preparation of 0.02N $C_2H_2O_4$ solution

For 100 mL of 1N $C_2H_2O_4$ solution, 6.36g of oxalic acid crystals were properly weighed and dissolved in distilled water. In a 100 mL V.F, 2 mL of that 1N $C_2H_2O_4$ solution was diluted with distilled water to make 0.02N $C_2H_2O_4$ solution.

3.3.7 Preparation of NaOH solution

After examing with primary standard solution $C_2H_2O_4$, to make 5M NaOH solution, 20g of NaOH pellets were weighed and dissolved in 100 mL of distilled water. Other concentrations of NaOH were obtained as follows: 1M, 0.5M, 0.1M, 0.05M, and 0.01M from a 5M NaOH solution by dilution.

3.3.8 Preparation of buffer solution

Buffer solutions of pH 4.0, 7.0, and 9.2 were taken for pH meter calibration by dissolving the appropriate buffer tablets in distilled water in three separate volumetric flasks of 100 mL and diluting up to the mark.

3.3.9 Preparation of ascorbic acid

6g of ascorbic acid was weighed accurately to dissolve with 100 mL water along with 0.5 mL acetone.

3.4 Preparation of Fe(III)-loaded biosorbent from raw banana peel (BP)

3.4.1 Collection and pretreatment of raw banana peel

The raw banana peel was collected from Bhotahity, Kathmandu. The assembled peel was cleaned with water and dried for a week. The dry material was then crushed in a laboratory mill and sieved through a 150 μm sieve to yield fixed-sized particles. It was then kept in a clean, dry jar. As a result, the crushed powder was named as a raw biosorbent, abbreviated as RBP.

3.4.2 Preparation of saponified Fe(III)-loaded raw banana peel

100 g of RBP was weighed and added with 8 g of $Ca(OH)_2$ powder with 2 pellets of NaOH in a 500 mL beaker. Then it was stirred in a magnetic stirrer for 24h. It was filtered and the residue was washed till neutral. The sample was then dried for 24h. The temperature was maintained at 70°C for 24 hour. Thus obtained sample is known as saponified BP called SBP. 5g SBP was mixed with 500 mL of 0.01 M $FeCl_3$ for Fe(III)-loading. The pH during loading was maintained at 3. Then it was shaken for 24 hour. It was filtered and the residue was washed till neutral. The sample was then dried for 24h which was named as Fe(III)-SBP hereafter.

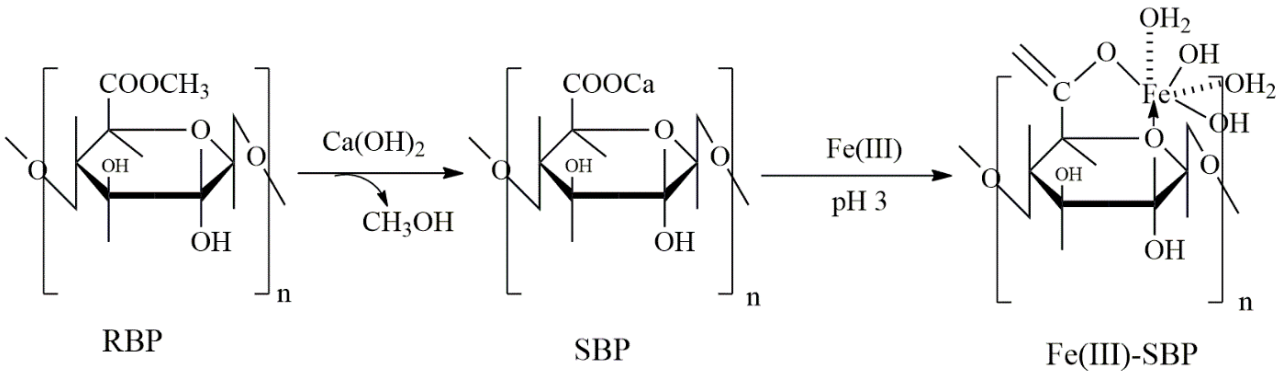

Scheme 3.1: Synthetic route of Fe(III)-SBP from RBP by saponification process followed by Fe-loading

Scheme 3.1 shows that -CH_3 group from -$COOCH_3$ of pyranose ring is replaced by Ca on the elimination of CH_3OH termed as SBP. Fe(III) is coordinated to 2(-OH), 2(-OH_2),1 O atom of pyranose ring and 1 O atom outside the ring termed as Fe(III)-SBP. The pH was maintained at 3 during Fe(III) loading.

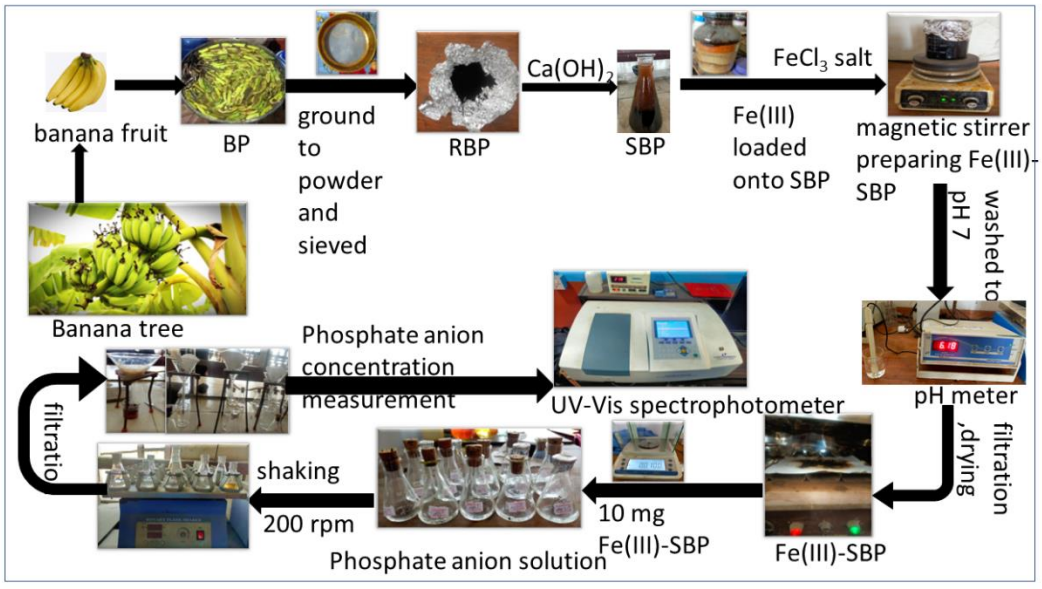

Scheme 3.2: Flow chart showing the details of the biosorbent synthetic route from banana peel loading Fe(III) for the biosorption of phosphate from aqueous solution.

Scheme 3.2 shows the laboratory activities carried out at Chemistry Department, Amrit Campus. At first banana peels (BP) were collected from the juice shop. BP were dried for 10 days and ground to fine powder named as raw banana powder (RBP). RBP was sieved followed by washing with rain water. It was dried under sun for 3 days and in oven for 24h. RBP was treated with $Ca(OH)_2$ to get SBP. SBP was followed by Fe(III)-loading. The residue was washed until neutral, filtered and dried. The outcome is termed as Fe(III)-SBP. SBP and Fe(III)-SBP were measured and treated with phosphate solution. They were rotated in shaker. The solution was filtered. The solution concentration prior to and after shaking were determined by UV-Vis spectrophotometer.

3.5 Colour development by molybdenum blue method

The spectrophotometric approach needs the creation of colour. It was used to analyze the concentration of PO_4^{3-}. In 2.5 mL sample of PO_4^{3-}, 2 mL of mixture of ammonium molybdate and $K_2(SbO)_2C_8H_4O_{10}.3H_2O$ was added. Then 2 mL of ascorbic acid followed by 1 mL of 5N H_2SO_4 was kept. The solution was kept in dark for 25 minutes till the complete development of colour. Then PO_4^{3-} concentration was then measured with UV-Vis spectrophotometer.

3.6 Preparation of calibration curve for spectrophotometric determination of PO_4^{3-}

For a calibration curve, PO_4^{3-} solutions with different concentrations of 0.5, 1, 2, 3, 4, 5, 6, 7, 8, 9, and 10 mg/L exactly were made from stock solution by serial dilution and their absorbance was measured with a spectrophotometer at λ_{max} (850 nm). A graph of absorbance *vsersus* PO_4^{3-}concentration was plotted. Slope was calculated from the straight line and it was used to calculate the unknown concentration of PO_4^{3-} in the solution.

3.7 Determination of pHpzc

The pH of the suspension medium at which particles have no surface charge (pHpzc) is important in understanding biosorption processes. At pH<pHpzc, the surface has a

net positive charge, which promotes anion biosorption, whereas at pH>pHpzc, the surface has a net negative charge, which promotes cation biosorption.

0.01M, 0.05M, and 0.1M of NaCl solution in 50 mL volumetric flask were prepared. Then 50 mg of Fe(III)-SBP with 10 ml of 0.01M NaCl at varying pH (1-12) was shaken for 24 h. Initial and final pH were measured. The experiment was repeated for 0.05M and 0. 1M NaCl solution. The plot of ΔpH *versus* initial pH for all three solutions were done. The point where pH change is zero indicates pHpzc.

3.8 Desorption test

50 mg of the biosorbent consisting of PO_4^{3-} [Fe(III)-SBP@PO_4] was desorbed using 10 mL NaOH of different concentration.

3.9 Co-existing ions

Various salt solution containing Cl^-, NO_3^-, CO_3^{--}, HCO_3^- and SO_4^{--} were used to observe the effects onto biosorption of phosphate. Five solutions of 0, 10, 50, 100 and 200 mg/L were prepared. In order to prepare a solution of 200, 100, 50, 10 and 0 mg/L (20 mL), phosphate solution of concentration 50 mg/L (4 mL), corresponding salt (Cl^-, NO_3^-, CO_3^{--}, HCO_3^-, SO_4^{--}) of 250 mg/L (16, 12, 8, 4, 0.8 and 0 mL respectively) and remaining volume of water was added together. In this way a 20 mL of solution was prepared. Then pH of 20 mL solution was made at optimum. Each solution was shaken with 10 mg Fe(III)-SBP and their concentration was measured before and after biosorpion. The effect of five solutions onto the biosorption of phosphate was observed.

3.10 Characterization Techniques:

3.10.1 Fourier transform infrared (FTIR) spectroscopy

The FTIR technique is very sensitive, a simple non-destructive technology based on the absorption intensities of various functional groups at different wavenumbers in the near-infrared region, notably carboxylate (COO^-) and ester carbonyl (C=O) groups. This work employed Fourier transform infrared (FTIR) spectroscopy to describe distinct functional groups in RBP, SBP, and Fe(III)-SBP. In tiny vials, single particle of RBP, SBP, and Fe(III)-SBP was placed, and FTIR analysis was performed at Amrit Campus in Lainchaur, Thamel.

3.10.2 Energy dispersive X-ray (EDX) Analysis

EDX spectroscopy determines the elemental composition of a specimen by detecting the X-ray emitted by the sample. EDX spectroscopy can detect elements with atomic numbers greater than boron at concentrations as low as 0.1% and can be used for material evaluation and identification, contamination identification, spot detection analysis of regions up to 10 cm in diameter. Energy dispersive X-ray was employed to study the surface morphology, microstructure and elemental composition of our sample (Fe(III)-SBP-PO_4) at Jeonbuk National University, Department of BIN Convergence Technology in Jeonju, South Korea.

3.10.3 Scanning electron microscopy (SEM) analysis

Scanning electron microscopy (SEM) is an electron microscopy technique that employs a focused beam of electrons that reacts with a sample to produce secondary electrons, backscattered electrons, and x-rays, which are then analysed to provide a topographical image and relative composition of the sample under investigation. SEM of phosphate-loaded Fe(III)-SBP was performed at Jeonbuk National University, Department of BIN Convergence Technology in Jeonju, South Korea.

CHAPTER IV

RESULTS AND DISCUSSION

4.1 Characterization of biosorbent

4.1.1 Scanning electron microscopy (SEM) analysis

SEM images of RBP, SBP and Fe(III)-SBP prior to and after phosphate biosorption were imaged to assess the surface morphology as shown in **Fig. 4.1 (a), (b),** and **(c)**. The surface of RBP is smooth with white patches (**Fig**. **4.1 a**). It is due to existence of soluble sugars, and low molecular weight organic compounds which is anticipated to be leached out after $Ca(OH)_2$ treatments. The surface of Fe(III)-SBP (**Fig. 4.1 b**) is rough and has uneven protuberances. The Fe(III)-SBP surface became uniform and smooth (**Fig. 4.1 c**) after phosphate biosorption which can be properly attributed due to coating of phosphate species onto Fe(III)-SBP surface.

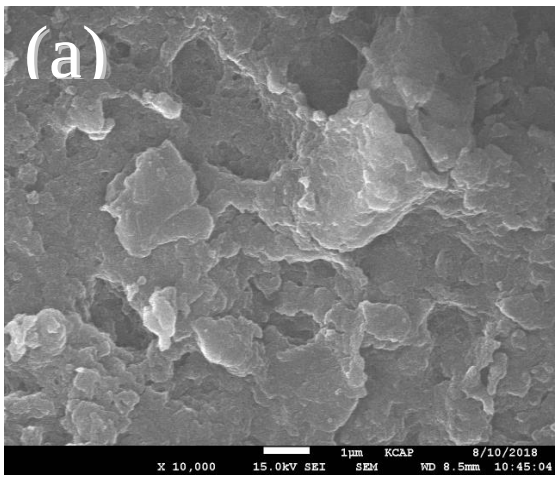

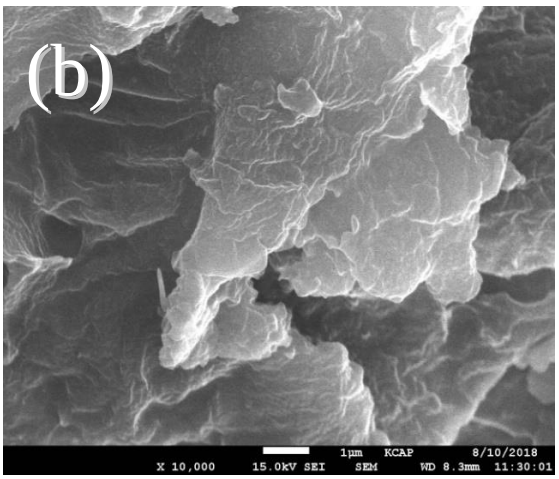

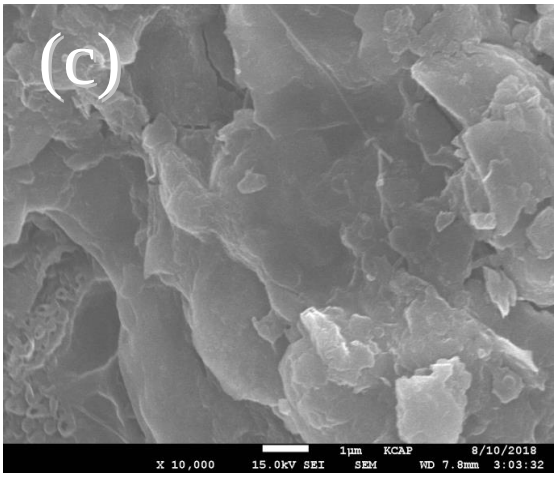

Figure 4.1: SEM images of a) RBP, b) Fe(III)-SBP and c) Fe(III)-SBP@PO_4

4.1.2 Functional groups analysis using FTIR spectroscopy

Fourier-transform infrared spectroscopy (FTIR) was used to screen the distinctive functional groups present on the surface of RBP, SBP, and Fe(III)-SBP in the spectral range of 4000 – 400 cm^{-1} as shown in **Fig. 4.2**. The strong peak observed at 3348 cm^{-1} in RBP which is due to -OH stretching vibration of cellulose, hemicellulose, pectin and lignin present in banana peel analog. The peak around 2923 cm^{-1} is due to bond stretching vibrations of methyl and methoxy groups. The peak around 1735 cm^{-1} is attributed due to -C=O stretching vibrations of carboxylic acids and esters. Small peaks around 1622, 1282 cm^{-1} may be attributed due to C-O stretching vibrations of carboxylic acids and alcohols. After $Ca(OH)_2$ treatments, the peak observed at around 1735 cm^{-1} is largely diminished in Fe(III)-SBP at around 1625 cm^{-1} is due to formation of Fe(III)- pectate. After phosphate biosorption, the peak at 3303 cm^{-1} (OH-stretching vibration) was found to be reduced in intensity. It was probably due to the involvement of -OH groups for phosphate biosorption. Similarly, the peak observed at around 1016 cm^{-1} (Turowski *et al.*, 1994) for Fe-O-P vibration, indicating that -OH group was replaced by the PO_4^{3-} anion. The peak observed at 1242 cm^{-1} is due to P-O stretching.

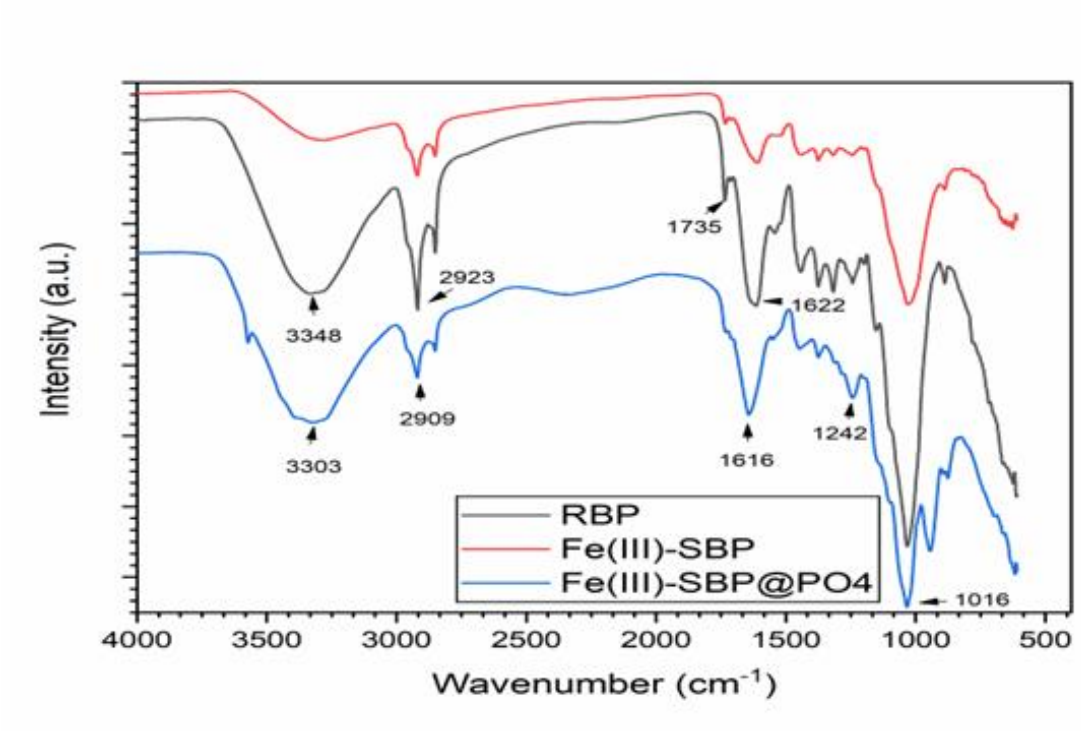

Figure 4.2: FTIR spectra of RBP, Fe(III)-SBP and Fe(III)-SBP@PO_4

4.1.3 Energy dispersive X-ray (EDX) analysis

EDX spectra of SBP, Fe(III)-SBP, and Fe(III)-SBP@PO_4 were recorded in order to investigate the elemental composition of the biosorbent, as reported in **Table 4.1**. The elemental composition of Fe(III)-SBP showed the proportion of new element Fe(III) to be 23.45% and the percentage of calcium was reduced from 23.94% to 1.882%. This finding demonstrated the successful loading of Fe(III) replacing Ca(II) from SBP *via* cation exchange mechanism. The weight ratio of Ca in (Fe(III)-SBP to SBP) is less than one (0.078) and that of Fe increment by 23.45. Similarly P had a weight ratio of 6.676 in Fe(III)-SBP@PO_4. This result showed that PO_4^{3-} was biosorbed onto Fe(III)-SBP effectively. This study demonstrated that Fe(III) was effectively loaded onto SBP which acts as anion exchanger, thereby biosorption of PO_4^{3-} occurs through ligand exchange mechanism.

Table 4.1: Elemental composition of SBP, Fe(III)-SBP and Fe(III)-SBP@PO_4

Elements	B.E (keV)	% weight SBP	% weight Fe(III)-SBP	weight ratio (Fe(III)-SBP to SBP)	% weight Fe(III)-SBP@PO_4	weight ratio (Fe(III)-SBP@PO_4 to Fe(III)-SBP)
C	0.27	55.038	54.42	0.988	42.12	0.774
O	0.52	18.30	18.02	0.984	32.42	1.81
P	2.01	ND	ND	-	6.676	6.676
Si	1.73	0.26	0.212	0.815	1.016	4.81
K	3.31	2.462	2.016	0.818	3.803	1.88
Ca	3.69	23.94	1.882	0.078	2.439	1.296
Fe	6.41	ND	23.450	23.45	11.526	0.491
Total		100.00	100.00		100.00	

4.1.4 Surface charge of the biosorbent

The point of zero charge of Fe(III)-SBP is one way to understand the biosorption mechanisms of phosphate anion. The surface charge of Fe(III)-SBP was evaluated by measuring the ΔpH at different initial pH as shown in **Fig**. **4.3**. The pH_{pzc} value obtained for Fe(III)-SBP is at 6.8. At pH_{pzc}, the surface charge of Fe(III)-SBP is neutral. At pH below pHpzc, the surface charge of biosorbent is positive due to

protonation. It was expected that the biosorption of phosphate anion can occur at the lower pH due to electrostatic interaction between phosphate anion and biosorbent surface. At pH closer to pH_{pzc}, the phosphate anions of aqueous solution substituted hydroxyl ligands of the coordination spheres of Fe(III)-SBP through ligand exchange mechanism. At pH greater than pH_{pzc}, the surface charge of biosorbent is negatively charged as a result of the electrostatic repulsion between negatively charged Fe(III)-SBP and phosphate anions led to poor biosorption of phosphate.

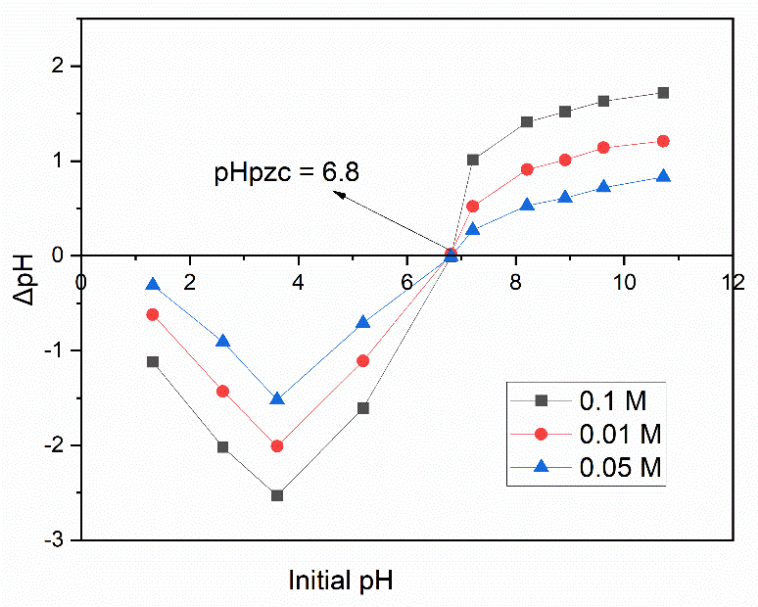

Figure 4.3: Determination of point zero charge (pH_{pzc}) for Fe(III)-SBP

4.2 Determination of λ_{max} and construction of calibration curve

Absorbance of solution was measured at different wave length. The plot of absorbance *versus* wave length was done to find the λ_{max} value. λ_{max} is the highest wavelength absorbed by the PO_4^{3-}. The λ_{max} value was found to be 850 nm which is similar as found in the literature (Malik *et al.*, 2021).

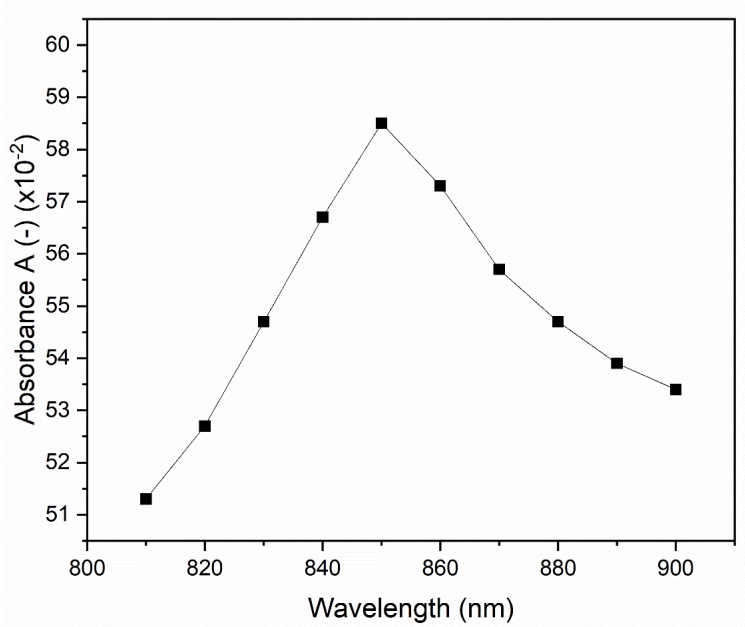

Figure 4.4: Determination of λ_{max}

Fig. 4.4 shows absorbance from 810 nm to 900 nm, in which maximum absorbance (λ_{max}) was obtained at 850 nm. Hence, λ_{max} of PO_4^{3-} was fixed at 850 nm for further examinations during the measurement of concentration of PO_4^{3-}.

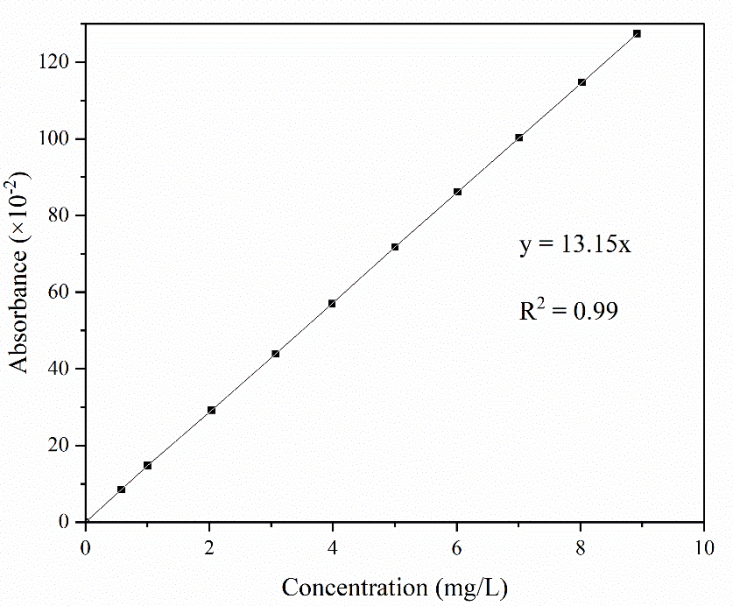

Figure 4.5: Calibration curve of PO_4^{---} at λ_{max}

Fig. 4.5 shows concentration of PO_4^{3-} *versus* absorbance. The slope 54.88 is shown in the graph. The concentration of given solution prior to and after biosorption were then calculated.

λ_{max} was fixed at 850 nm, a calibration curve was constructed by varying the concentration of the PO_4^{---} solution. When absorbance *versus* concentration was plotted, a linear line was obtained. It obeyed Lambert-Beer's law. Absorbance increased with an increase in the concentration of phosphate solution. It means absorbance is directly proportional to the concentration of phosphate solution because of increasing the concentration of $[H_4PMo(VI)_8Mo(V)_4O_{40}]^{3-}$. The concentration of unknown phosphate samples can be determined by using this calibration curve.

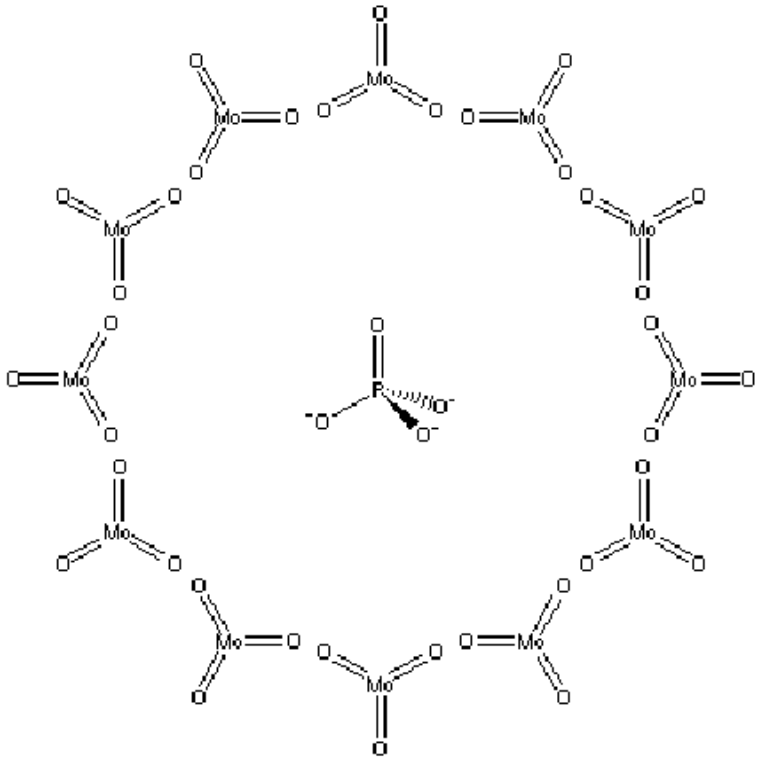

Figure 4.6: Molybdenum blue with central phosphate molecule (Omae *et al.*, 2007)

Fig 4.6 shows the structure of $[H_4PMo(VI)_8Mo(V)_4O_{40}]^{3-}$. It consists of Mo atom bonded with O atom. The structure shows the central PO_4^{---}.

4.3 Batch studies

4.3.1 Influence of the pH

The biosorption of phosphate anion is significantly influenced by both the surface charge of the biosorbent and the chemistry of the solution. The biosorption performance of RBP and Fe(III)-SBP is shown in **Fig. 4.7**. It showed that % biosorption of phosphate onto RBP increased from 3.6 % at pH 1.5 to 22% at pH 5.34. The Fe(III)- SBP biosorbent exhibits greater efficacy for the biosorption of phosphate which is 7.06 % at pH 1.5 to 88.80 % at pH 5.34. After pH 5.34, biosorption of phosphate in both biosorbents gradually decreases. The optimum pH for the biosorption of phosphate was evaluated to be 5.34. At pH closer to 5.34 biosorption of phosphate onto the biosorbent took place through electrostatic interaction as well as ligand exchange mechanism. At higher pH, due to electrostatic repulsion of hydroxyl ions with phosphate ions, poor biosorption of phosphate anions took place.

Table 4.2: % biosorption of RBP and Fe(III)-SBP at equilibrium pH

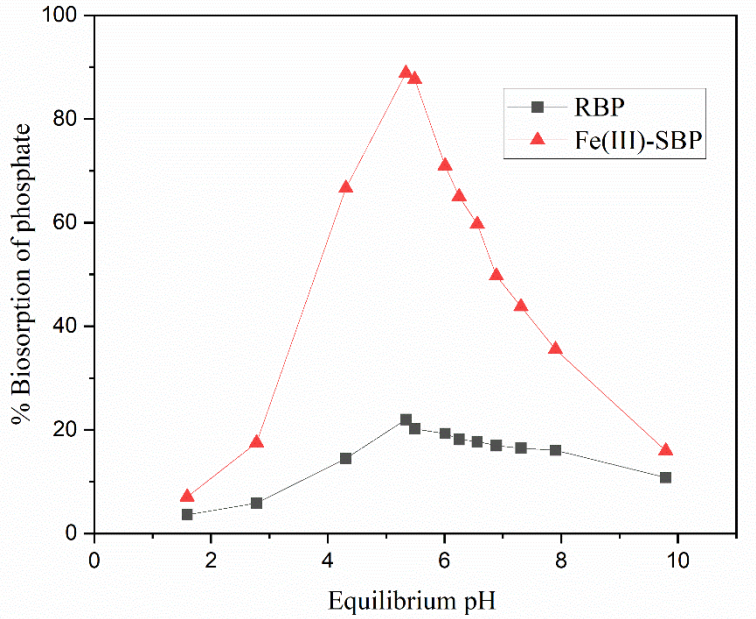

pHe	RBP	Fe(III)-SBP
1.5	3.6%	7.06 %
5.34	22%	88.80 %
9.7	10.81%	15.9%

Figure 4.7: Influence of pH for the biosorption of phosphate onto Fe(III)-SBP

4.3.2 Influence of contact time

Since RBP exhibited insignificant biosorption of phosphate over the whole pH range examined. The findings of the kinetic studies of Fe(III)-SBP at pH 5.34 are given in **Fig. 4.8**. **Fig. 4.8(a)** showed the progressive rise in the phosphate biosorption with increasing contact time in the early stage, then slowed down and again finally achieved plateau at 6 hours. The non-liner plot of experimental data, PFO and PSO data were shown in **Fig. 4.8(b)**. It showed that the PSO model closely validate with the experimental data. The result analysis of the PFO kinetic model is shown in **Fig. 4.8(c)** and PSO model in **Fig. 4.8(d)**. It showed that PSO kinetic model better fit the experimental data with higher coefficient of determination (0.989) than PFO model.

In addition, the rate constant and uptake capacity (q_e) was calculated and are shown in **Table 4.3** The value of q_e (4.032 mg/g) calculated from the PSO model is closer to the empirically observed q_e (3.91 mg/g) than that of the PFO model (Lin *et al.*, 2009). The phosphate biosorption onto Fe(III)-SBP followed a PSO kinetics. Therefore, chemisorption process is involved for the biosorption of phosphate onto Fe(III)-SBP (Manobala *et al.*, 2021).

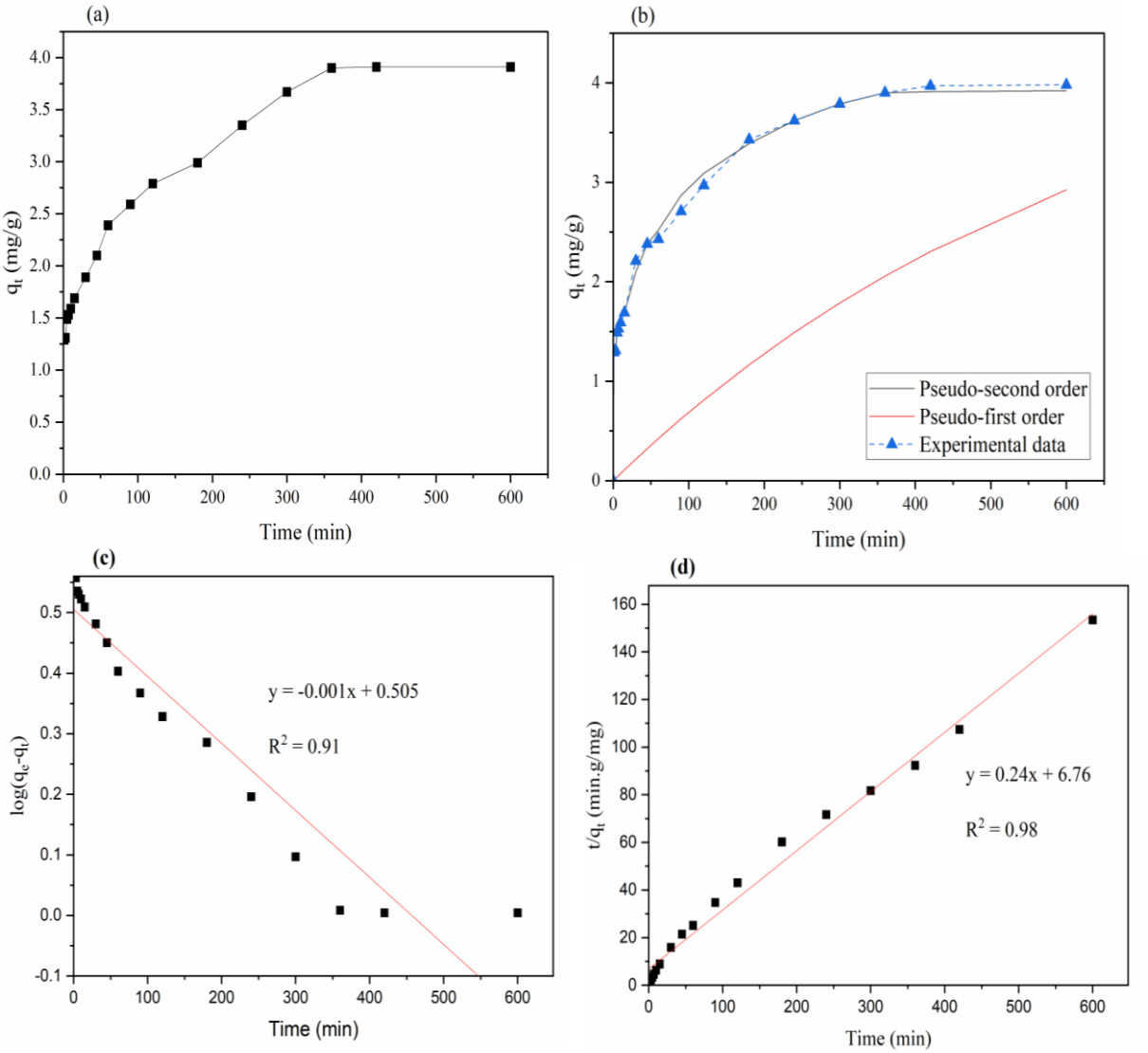

Figure 4.8: Biosorption of phosphate onto Fe(III)-SBP (a) Influence of contact time (b) Non-linear kinetics of phosphate biosorption onto Fe(III)-SBP (c) Plot of pseudo-first-order and (d) pseudo-second-order model

Table 4.3: Kinetic parameters for the biosorption of phosphate onto Fe(III)-SBP

Kinetic models	**Parameters**	**Values**
Pseudo-first-order	K_1 x 10^{-3} (min^{-1})	2.533
	q_e, cal. (mg/g)	0.505
	R^2	0.912
Pseudo-second-order	K_2 x 10^{-3} (g/mg min)	9.098
	q_e, exp. (mg/g)	3.91
	R^2	0.989
	q_e, exp. (mg/g)	3.91

4.3.3 Biosorption isotherms studies

The biosorption isotherm represents the relationship between the amount of sorbate biosorbed onto investigated biosorbent with the residual concentration of phosphate. **Fig. 4.9** showed the biosorption isotherm of phosphate using Fe(III)-SBP. As shown in **Fig. 4.9(a)** the phosphate biosorption onto Fe(III)-SBP increases at lower concentration whereas it is found to attain plateau value at higher concentration. **Fig. 4.9(b)** showed that the experimental data is in the same line with the Langmuir isotherm model. To analyse the best fit model, the experimental data were modelled using Langmuir isotherm **Fig. 4.9(c)** and Freundlich isotherms **Fig. 4.9(d)**. The results indicated that the data fitted well with the Langmuir isotherm model with high coefficient of determination (R^2 = 0.982) in comparison with Freundlich isotherm model (R^2 =0.910). **Table 4.4** displayed the computed isotherm parameters and coefficient of determination (R^2). The maximum monolayer biosorption capacity (q_{max}) of Fe(III)-SBP is calculated to be 18.51 mg/g which is very similar to the experimental value (17.31 mg/g) that is directly acquired through the plateau region in **Fig. 4.9(a).**

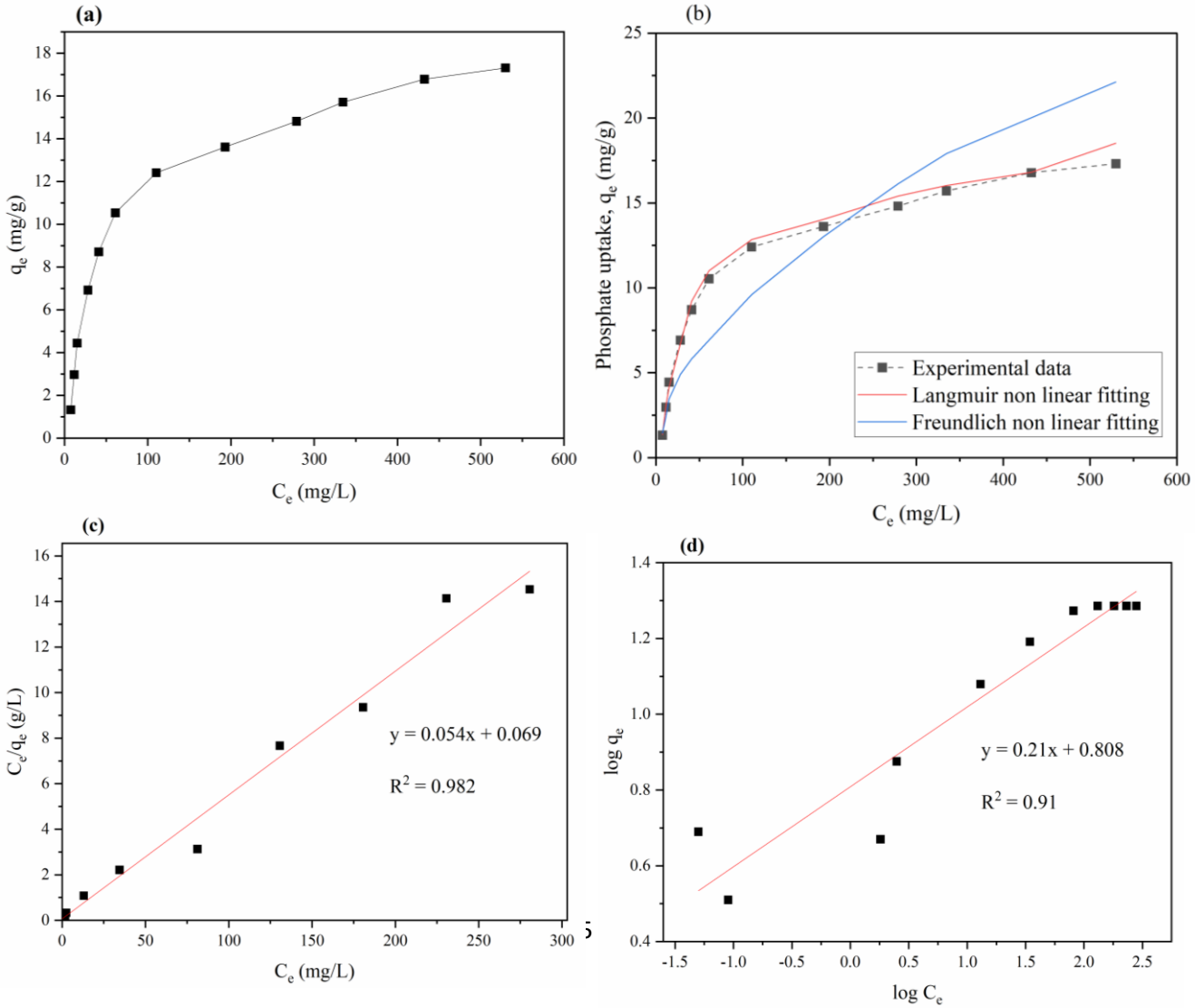

Figure 4.9: (a) Influence of initial concentration (b) non-linear isotherm of phosphate biosorption onto Fe(III)-SBP (c) Langmuir isotherm (d) Freundlich isotherm

Table 4.4: Isotherm parameters for the phosphate biosorption onto Fe(III)-SBP

Models	**Parameters**	**Values**
Langmuir	Qm, cal. (mg/g)	18.51
	b (L/mg)	0.78
	R^2	0.98
Freundlich	K_F (mg/g)	5.5
	1/n	0.24
	R^2	0.91

Table 4.5: Comparision of uptake capacity of Fe(III)-SBP with other biosorbents

Adsorbents	**q_{max} (mg/g)**	**References**
Zr(IV)-SOW	13.94	Biplov *et al*., 2008
Zr(IV)-SWR	27.63	Aryal *et al*., 2022
Zr-MCM 41	3.36	Jutidamrongphan *et al.*, 2012
Modified almond wooden shell	22.73	Faraj *et al*., 2020
La(III)-modifed Pine needles	4.8	Wang *et al*., 2015
Fe-loaded activated carbon	2.87	Barun *et al*., 2019
Fe(III)-SBP	18.51	This study

To evaluate the potentiality of investigated biosorbent, the maximum biosorption capacity of Fe(III)-SBP for phosphate is made analogous with some other biosorbents studied in the works of literature Biplov *et al*., (2008), Aryal *et al.,* (2022), Jutidamrongphan *et al.*, (2012), Faraj *et al*., (2020), Wang *et al*., (2015), Barun *et al*., (2019) as listed in **Table 4.5**. A comparison of the phosphate biosorption capacity of Fe(III)-SBP with other bio/adsorbents reveals higher biosorption capability than Zr(IV)-SOW, Zr-MCM 41, La(III)-modified pine needles and Fe-loaded activated carbon.

4.4 Influence of interfering anions

Natural wastewaters may contain a variety of ions such as HCO_3^-, CO_3^-, Cl^-, NO_3^- and SO_4^{--}, which can interfere for the biosorption of PO_4^{3-}anion. **Fig. 4.10** showed the effect of interfering ions for the biosorption of PO_4^{3-}anions. As concentration of interfering ions increases, % biosorption of PO_4^{3-} ion gradually decreased from 87.71% to 43.31%. The increased concentrations of HCO_3^-, CO_3^-, Cl^-, NO_3^- and SO_4^{--} inhibited PO_4^{3-} biosorption. SO_4^{--} interfered significantly with increase in concentration to 43.31%. The reason behind highest interference caused by SO_4^{--} is due to more charge density of SO_4^{--}. SO_4^{--} is divalent and has stronger interferences than any of the other interfering ions.

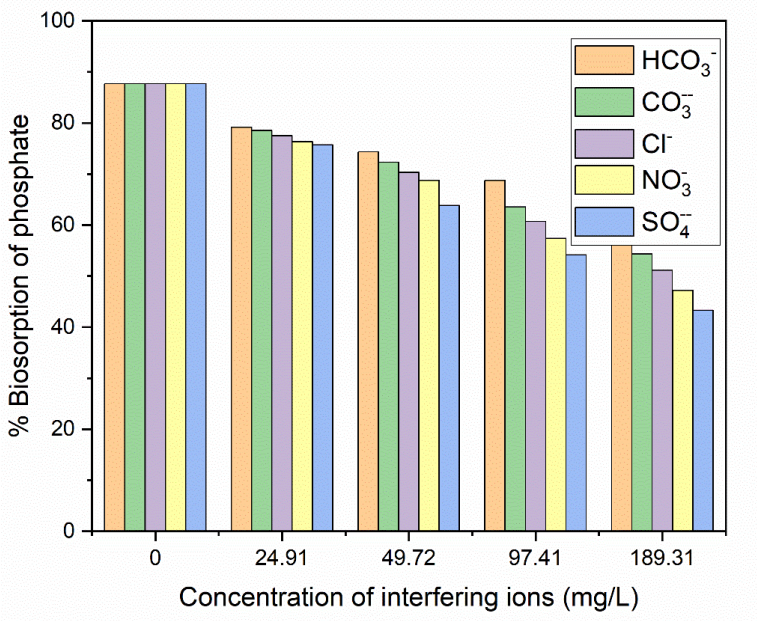

Figure 4.10: Influence of interfering anions in the biosorption of phosphate onto Fe(III)-SBP

4.5 Phosphate biosorption mechanism

Stable Fe(III) chelate of pectic acid with five-membered ring is inferred to be formed in the interaction of banana pectic acid with Fe(III). In Fe(III) loaded SBP, all the positive charge of the loaded Fe(III) ions is impossible to be neutralized by carboxylic groups due to the large steric hindrance by big polymeric chains of banana pectic acid. So that, only one or two positive charge of the loaded Fe(III) ions are neutralized by carboxylic group of banana pectic acid, and other positive charges are neutralized by anionic species like hydroxyl or chloride ions existing in the aqueous solution. These hydroxyl/chloride ligand undergo ligand exchange reaction with phosphate anion during biosorption.

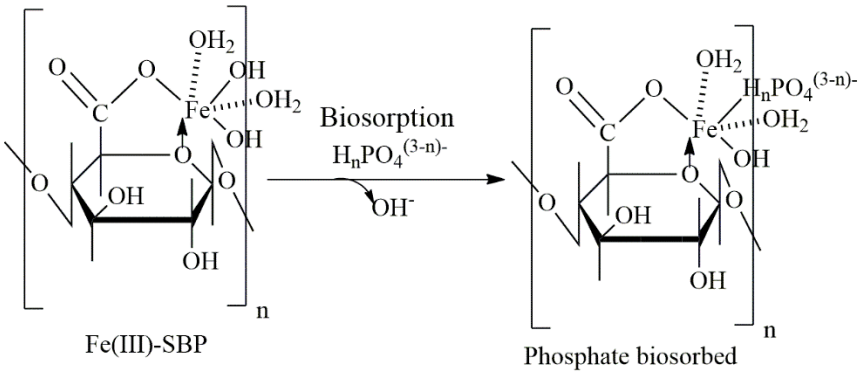

Scheme 4.1: Inferred mechanism of phosphate biosorption onto Fe(III)-SBP biosorbent

Scheme 4.1 shows Fe(III)-SBP and phosphate biosorbed Fe(III)-SBP. Fe(III)-SBP undergoes ligand exchange mechanism. (-OH) group of Fe(III)-SBP is replaced by $H_nPO_4^{(3-n)-}$ which is present in the aqueous solution, where n = 1 or 2. In this way, phosphate ion is biosorbed by the biosorbent.

4.6 Desorption studies

The desorption studies is crucial to recover biosorbed sorbate and regenerate the biosorbent. The desorption experiment was carried in basic medium. Different concentration of NaOH of 0.01, 0.1, 0.2, 0.5 and 1M were used in the desorption experiments as shown in **Fig. 4.11**. The findings showed that increment in NaOH concentrations from 0.01 to 0.5M, phosphate desorption also gradually decreases from 53.21 to 93.34 %. However, desorption of biosorbed phosphate decreases with 1M NaOH due to rupture of surface area of Fe(III)-SBP.

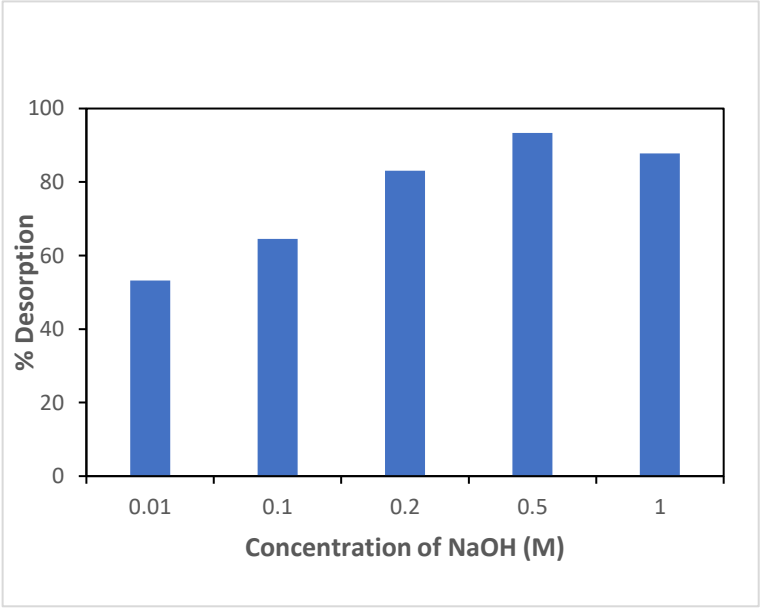

Figure 4.11: Desorption of phosphate biosorbed Fe(III)-SBP as a function of NaOH concentration.

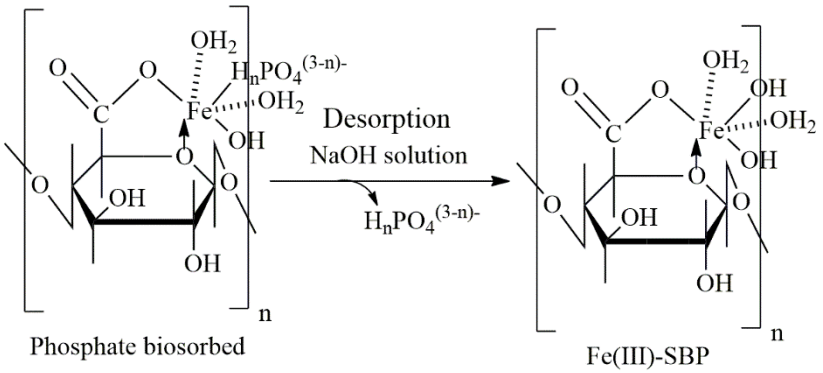

Scheme 4.2: Inferred mechanism of phosphate desorption using NaOH solution (Gu *et al.*, 2019)

Scheme 4.2 shows the biosorbed phosphate anion can be easily desorbed with NaOH by the ligand exchange mechanism between the biosorbed phosphate anions and high concentration of OH^- ions present in the solution.

CHAPTER V

CONCLUSIONS, LIMITATION AND SUGGESTIONS

5.1 Conclusions

Phosphate bisorption from aqueous solution was investigated using Fe(III)-SBP as the biosorbent. To prepare Fe(III)-SBP, banana peel was saponified with $Ca(OH)_2$ and then loaded with Fe(III). SEM analysis showed the altered morphology of Fe(III)-SBP prior to and after biosorption. EDX analysis indicated the increment in Ca(II), Fe(III) and phosphate in SBP, Fe(III)-SBP and biosorbed Fe(III)-SBP. FTIR analysis indicated the principal role of carboxyl functional group for biosorption. The effects of pH, biosorption isotherms, kinetic investigations, and interfering ions on phosphate biosorption were investigated. The examined biosorbent's point of zero charges (pH_{PZC}) was determined to be 6.8. The highest phosphate loading of Fe(III)-SBP calculated using the Langmuir isotherm model was 18.51 mg/g. The Langmuir isotherm model, which represents phosphate monolayer biosorption, can better explain the biosorption of phosphate onto Fe(III)-SBP. Kinetic analysis showed PSO kinetic model suited the experimental data well. Various anions, such as Cl^- and NO_3^-, have no appreciable influence; nevertheless, SO_4^{--} has maximum interference. Using a 0.5M NaOH, the biosorbed phosphate was successfully eluted. Compared to reported biosorbents, Fe(III)-SBP has superior phosphate biosorption performance. The experimental findings showed that Fe(III)-SBP can be an efficient and low-cost material for phosphate biosorption from aqueous solution.

5.2 Limitations of the study

a. Before the experiment, no additional purification of the chemicals was performed.

b. Many advanced technologies such as ICP-MS, XPS, and XRD measurement, were not used.

c. Phosphate was not a hundred percent removed.

d. Research on factors like the impact of temperature and agitation speed hasn't been done.

e. The elution study was only done using NaOH as an eluent.

f. Biosorption and desorption cycles for phosphate ion were not tested.

g. All the experiments were carried out in laboratory conditions.

5.3 Suggestion for further works

a. Variation of the adsorption capacity at different temperature can be done.
b. Advanced characterization technologies such as ICP-MS, AAS, TEM and XPS can be used for further information.
c. For evaluating repeated usage and durability (adsorbent cycle test) can be conducted.
d. A desorption study can be done by using other possible eluents.
e. Column studies for biosorption of phosphate can be performed.

REFERENCES

Ade, P. A., Aghanim, N., Argueso, F., Armitage-Caplan, C., Arnaud, M., Ashdown, M., Atrio-Barandela, F., Aumont, J., Baccigalupi, C., Banday, A.J., Barreiro, R.B., & Munshi, D. (2014). Planck 2013 results. XXVIII. The Planck catalogue of compact sources. *Astronomy & Astrophysics*, **571**, A28.

Ahmad, M., Moon, D. H., Vithanage, M., Koutsospyros, A., Lee, S. S., Yang, J. E., & Ok, Y. S. (2014). Production and use of biochar from buffalo-weed (*Ambrosia trifida L.)* for trichloroethylene removal from water. *Journal of Chemical Technology & Biotechnology*, **89**(1), 150-157.

Ahmed, S. F., Mofijur, M., Nuzhat, S., Chowdhury, A. T., Rafa, N., Uddin, M. A., Inayat A., Mahlia, T.M., Ong, H.C., Chia, W.Y., & Show, P. L. (2021). Recent developments in physical, biological, chemical, and hybrid treatment techniques for removing emerging contaminants from wastewater. *Journal of Hazardous Materials*, **416**, 125912.

Akpomie, K. G., & Conradie, J. (2020). Banana peel as a biosorbent for the decontamination of water pollutants. A review. *Environmental Chemistry Letters*, **18**, 1085-1112.

Akram, M., Gao, B., Pan, J., Khan, R., Inam, M. A., Xu, X., & Yue, Q. (2022). Enhanced removal of phosphate using pomegranate peel-modified nickel lanthanum hydroxide. *Science of The Total Environment*, **809**, 151181.

Aktar, J. (2021). Batch adsorption process in water treatment. In *Intelligent Environmental Data Monitoring for Pollution Management* (pp. 1-24). Academic Press.

Ali, A., Saeed, K., & Mabood, F. (2016). Removal of chromium (VI) from aqueous medium using chemically modified banana peels as efficient low-cost adsorbent. *Alexandria Engineering Journal*, **55**(3), 2933-2942.

Ali, I. (2012). New generation adsorbents for water treatment. *Chemical Reviews*, **112**(10), 5073-5091..

Amela, K., Hassen, M. A., & Kerroum, D. (2012). Isotherm and kinetics study of biosorption of cationic dye onto banana peel. *Energy Procedia*, **19**, 286-295.

Annadurai, G., Juang, R. S., & Lee, D. J. (2002). Use of cellulose-based wastes for adsorption of dyes from aqueous solutions. *Journal of Hazardous Materials*, **92**(3), 263-274.

Arami, M., Limaee, N. Y., Mahmoodi, N. M., & Tabrizi, N. S. (2006). Equilibrium and kinetics studies for the adsorption of direct and acid dyes from aqueous solution by soy meal hull. *Journal of Hazardous Materials*, **135**(1-3), 171-179.

Aryal, M., & Liakopoulou-Kyriakides, M. (2011). Equilibrium, kinetics and thermodynamic studies on phosphate biosorption from aqueous solutions by Fe (III)-treated *Staphylococus xylosus* biomass: Common ion effect. *Colloids and Surfaces A: Physicochemical and Engineering Aspects*, **387**(1-3), 43-49.

Aryal, M., Ziagova, M., & Liakopoulou-Kyriakides, M. (2010). Study on arsenic biosorption using Fe(III)-treated biomass of *Staphylococcus xylosus*. *Chemical Engineering Journal*, **162**(1), 178-185.

Aryal, R. L., Bhurtel, K. P., Poudel, B. R., Pokhrel, M. R., Paudyal, H., & Ghimire, K. N. (2022). Sequestration of phosphate from water onto modified watermelon waste loaded with Zr (IV). *Separation Science and Technology*, **57**(1), 70-82.

Aryal, R. L., Thapa, A., Poudel, B. R., Pokhrel, M. R., Dahal, B., Paudyal, H., & Ghimire, K. N. (2022). Effective biosorption of arsenic from water using La(III) loaded carboxyl functionalized watermelon rind. *Arabian Journal of Chemistry*, **15**(3), 103674.

Ashokkumar, K., Elayabalan, S., Shobana, V. G., Sivakumar, P., & Pandiyan, M. (2018). Nutritional value of cultivars of Banana (*Musa spp*.) and its future prospects. *Journal of Pharmacognosy and Phytochemistry*, **7**(3), 2972-2977.

Awual, M. R., El-Safty, S. A., & Jyo, A. (2011). Removal of trace arsenic(V) and phosphate from water by a highly selective ligand exchange adsorbent. *Journal of Environmental Sciences*, **23**(12), 1947-1954.

Awual, M. R., El-Safty, S. A., & Jyo, A. (2011). Removal of trace arsenic(V) and phosphate from water by a highly selective ligand exchange adsorbent. *Journal of Environmental Sciences*, **23**(12), 1947-1954.

Ayele, H. S., & Atlabachew, M. (2021). Review of characterization, factors, impacts, and solutions of Lake eutrophication: lesson for lake Tana,

Ethiopia. *Environmental Science and Pollution Research*, **28(**12), 14233-14252.

Bacelo, H., Pintor, A. M., Santos, S. C., Boaventura, R. A., & Botelho, C. M. (2020). Performance and prospects of different adsorbents for phosphorus uptake and recovery from water. *Chemical Engineering Journal*, **381**, 122566.

Banu, H. A. T., Karthikeyan, P., & Meenakshi, S. (2019). Comparative studies on revival of nitrate and phosphate ions using quaternized corn husk and jackfruit peel. *Bioresource Technology Reports*, **8**, 100331.

Bellahsen, N., Kakuk, B., Beszédes, S., Bagi, Z., Halyag, N., Gyulavari, T., & Hodur, C. (2021). Iron-loaded pomegranate peel as a bio-adsorbent for phosphate removal. *Water*, **13**(19), 2709.

Bijekar, S., Padariya, H. D., Yadav, V. K., Gacem, A., Hasan, M. A., Awwad, N. S., & Jeon, B. H. (2022). The state of the art and emerging trends in the wastewater treatment in developing nations. *Water*, **14**(16), 2537.

Biswas, B. K., Inoue, K., Ghimire, K. N., Harada, H., Ohto, K., & Kawakita, H. (2008). Removal and recovery of phosphorus from water by means of adsorption onto orange waste gel loaded with zirconium. *Bioresource Technology*, **99**(18), 8685-8690.

Biswas, B. K., Inoue, K., Ghimire, K. N., Ohta, S., Harada, H., Ohto, K., & Kawakita, H. (2007). The adsorption of phosphate from an aquatic environment using metal-loaded orange waste. *Journal of Colloid and Interface Science*, **312**(2), 214-223.

Blaney, L. M., Cinar, S., & SenGupta, A. K. (2007). Hybrid anion exchanger for trace phosphate removal from water and wastewater. *Water Research*, **41**(7), 1603-1613.

Bouamra, F., Drouiche, N., Abdi, N., Grib, H., Mameri, N., & Lounici, H. (2018). Removal of phosphate from wastewater by adsorption on marble waste: effect of process parameters and kinetic modeling. *International Journal of Environmental Research*, **12**, 13-27.

Bouamra, F., Drouiche, N., Abdi, N., Grib, H., Mameri, N., & Lounici, H. (2018). Removal of phosphate from wastewater by adsorption on marble waste: effect of process parameters and kinetic modeling. *International Journal of Environmental Research*, **12**, 13-27.

Brendonck, L., Maes, J., Rommens, W., Dekeza, N., Nhiwatiwa, T., Barson, M., & Marshall, B. (2003). The impact of water hyacinth (*Eichhornia crassipes*) in a eutrophic subtropical impoundment (Lake Chivero, Zimbabwe). II. Species diversity. *Archiv Fur Hydrobiologie*, **158**(3), 389-405.

Carvalho, W. S., Martins, D. F., Gomes, F. R., Leite, I. R., da Silva, L. G., Ruggiero, R., & Richter, E. M. (2011). Phosphate adsorption on chemically modified sugarcane bagasse fibres. *Biomass and Bioenergy*, **35**(9), 3913-3919.

Chen, Z., Wu, Y., Huang, Y., Song, L., Chen, H., Zhu, S., & Tang, C. (2022). Enhanced adsorption of phosphate on orange peel-based biochar activated by Ca/Zn composite: Adsorption efficiency and mechanisms. *Colloids and Surfaces A: Physicochemical and Engineering Aspects*, **651**, 129728.

Cid, C. A., Jasper, J. T., & Hoffmann, M. R. (2018). Phosphate recovery from human waste via the formation of hydroxyapatite during electrochemical wastewater treatment. *ACS Sustainable Chemistry & Engineering*, **6**(3), 3135-3142.

Cisse, L., & Mrabet, T. (2004). World phosphate production: overview and prospects. *Phosphorus Research Bulletin*, **15**, 21-25.

Clark, T., Stephenson, T., & Pearce, P. A. (1997). Phosphorus removal by chemical precipitation in a biological aerated filter. *Water Research*, **31**(10), 2557-2563.

Dokulil, M. T., & Teubner, K. (2011). Eutrophication and climate change: present situation and future scenarios. *Eutrophication: Causes, Consequences and Control*, 1-16.

Dong, J., Ma, G., Sui, L., Wei, M., Satheesh, V., Zhang, R., Ge, S., Li, J., Zhang, T.E., Wittwer, C. & Lei, M. (2019). Inositol pyrophosphate InsP8 acts as an intracellular phosphate signal in *Arabidopsis*. *Molecular Plant*, **12**(11), 1463-1473.

Fan, C., & Zhang, Y. (2018). Adsorption isotherms, kinetics and thermodynamics of nitrate and phosphate in binary systems on a novel adsorbent derived from corn stalks. *Journal of Geochemical Exploration*, **188**, 95-100.

Ganesh, S., Khan, F., Ahmed, M. K., Velavendan, P., Pandey, N. K., & Kamachi Mudali, U. (2012). Spectrophotometric determination of trace amounts of phosphate in water and soil. *Water Science and Technology*, **66**(12), 2653-2658.

Gao, Q., Wang, C. Z., Liu, S., Hanigan, D., Liu, S. T., & Zhao, H. Z. (2019). Ultrafiltration membrane microreactor (MMR) for simultaneous removal of nitrate and phosphate from water. *Chemical Engineering Journal*, **355**, 238-246.

Ghimire, K. N., Inoue, J. I., Inoue, K., Kawakita, H., & Ohto, K. (2008). Adsorptive separation of metal ions onto phosphorylated orange waste. *Separation Science and Technology*, **43**(2), 362-375.

Gkika, D. A., Mitropoulos, A. C., & Kyzas, G. Z. (2022). Why reuse spent adsorbents? The latest challenges and limitations. *Science of The Total Environment*, **822**, 153612.

Ghosh, S., Bhattacharya, J., Nitnavare, R., & Webster, T. J. (2022). Heavy metal removal by *Bacillus* for sustainable agriculture. In *Bacilli in Agrobiotechnology: Plant Stress Tolerance, Bioremediation, and Bioprospecting* (pp. 1-30). Cham: Springer International Publishing.

Guo, Y., Liu, C., Ye, R., & Duan, Q. (2020). Advances on water quality detection by uv-vis spectroscopy. *Applied sciences*, **10**(19), 6874.

Hameed, B. H., Ahmad, A. A., & Aziz, N. (2007). Isotherms, kinetics and thermodynamics of acid dye adsorption on activated palm ash. *Chemical Engineering Journal*, **133**(1-3), 195-203.

Hasan, Z., & Tewari, D. D. (2020). Characteristics of Groundwater Quality in the Aquifer of Indo-Nepal Border of Balrampur City. *International Journal of Plant and Environment*, **6**(02), 146-151.

Hashim, K. S., Al Khaddar, R., Jasim, N., Shaw, A., Phipps, D., Kot, P., Pedrola, M.O., Alattabi, A.W., Abdulredha, M & Alawsh, R. (2019). Electrocoagulation as a green technology for phosphate removal from River water. *Separation and Purification Technology*, **210**, 135-144.

Ho, Y. S., & McKay, G. (1998). Sorption of dye from aqueous solution by peat. *Chemical Engineering Journal*, **70**(2), 115-124.

Ho, Y. S., & McKay, G. (1999). Pseudo-second order model for sorption processes. *Process Biochemistry*, **34**(5), 451-465.

Huang, Y. D. (2022). Comments on using of “pseudo-first-order kinetic model”[Sci. Total Environ. 750 (2021) 142370, 750 (2021) 141498, 761 (2021) 143229]. *Science of The Total Environment*, **826**, 154291.

Lin, J., & Wang, L. (2009). Comparison between linear and non-linear forms of pseudo-first-order and pseudo-second-order adsorption kinetic models for the removal of methylene blue by activated carbon. *Frontiers of Environmental Science & Engineering in China*, **3**, 320-324.

Jiuhui, Q. U. (2008). Research progress of novel adsorption processes in water purification: a review. *Journal of Environmental Sciences*, **20**(1), 1-13.

Jung, K. W., Hwang, M. J., Ahn, K. H., & Ok, Y. S. (2015). Kinetic study on phosphate removal from aqueous solution by biochar derived from peanut shell as renewable adsorptive media. *International Journal of Environmental Science and Technology*, **12**, 3363-3372.

Jung, K. W., Jeong, T. U., Choi, J. W., Ahn, K. H., & Lee, S. H. (2017). Adsorption of phosphate from aqueous solution using electrochemically modified biochar calcium-alginate beads: Batch and fixed-bed column performance. *Bioresource Technology*, **244**, 23-32.

Kondalkar, M., Fegade, U., Attarde, S., & Ingle, S. (2019). Phosphate removal, mechanism, and adsorption properties of Fe-Mn-Zn oxide trimetal alloy nanocomposite fabricated via co-precipitation method. *Separation Science and Technology*, **54**(16), 2682-2694.

Krishnaprabu, S. (2020). Liquid microbial consortium: A potential tool for sustainable soil health. *Journal of Pharmacognosy and Phytochemistry*, **9**(2), 2191-2199.

Kumar, M., Badruzzaman, M., Adham, S., & Oppenheimer, J. (2007). Beneficial phosphate recovery from reverse osmosis (RO) concentrate of an integrated membrane system using polymeric ligand exchanger (PLE). *Water Research*, **41**(10), 2211-2219.

Kumar, P. S., Gayathri, R., & Rathi, B. S. (2021). A review on adsorptive separation of toxic metals from aquatic system using biochar produced from agro-waste. *Chemosphere*, **285**, 131438.

Kumar, P., Sudha, S., Chand, S., & Srivastava, V. C. (2010). Phosphate removal from aqueous solution using coir-pith activated carbon. *Separation Science and Technology*, **45**(10), 1463-1470.

Lacasa, E., Canizares, P., Saez, C., Fernandez, F. J., & Rodrigo, M. A. (2011). Electrochemical phosphates removal using iron and aluminium electrodes. *Chemical Engineering Journal*, **172**(1), 137-143.

Lee, B. J., Schlautman, M. A., Toorman, E., & Fettweis, M. (2012). Competition between kaolinite flocculation and stabilization in divalent cation solutions dosed with anionic polyacrylamides. *Water Research*, **46**(17), 5696-5706.

Li, J., Ianaiev, V., Huff, A., Zalusky, J., Ozersky, T., & Katsev, S. (2021). Benthic invaders control the phosphorus cycle in the world's largest freshwater ecosystem. *Proceedings of The National Academy of Sciences*, **118**(6), e2008223118.

Li, Q., Fu, L., Wang, Y., Zhou, D., & Rittmann, B. E. (2018). Excessive phosphorus caused inhibition and cell damage during heterotrophic growth of *Chlorella regularis*. *Bioresource Technology*, **268**, 266-270.

Li, X., Xie, Y., Jiang, F., Wang, B., Hu, Q., Tang, Y., Luo, T. & Wu, T. (2020). Enhanced phosphate removal from aqueous solution using resourceable nano-CaO_2/BC composite: Behaviors and mechanisms. *Science of The Total Environment*, **709**, 136123.

Liu, R., Chi, L., Wang, X., Sui, Y., Wang, Y., & Arandiyan, H. (2018). Review of metal (hydr) oxide and other adsorptive materials for phosphate removal from water. *Journal of Environmental Chemical Engineering*, **6**(4), 5269-5286.

Lou, K., Rajapaksha, A. U., Ok, Y. S., & Chang, S. X. (2016). Pyrolysis temperature and steam activation effects on sorption of phosphate on pine sawdust biochars in aqueous solutions. *Chemical Speciation & Bioavailability*, **28**(1-4), 42-50.

Madhav, S., Ahamad, A., Singh, A. K., Kushawaha, J., Chauhan, J. S., Sharma, S., & Singh, P. (2020). Water pollutants: sources and impact on the environment and human health. *Sensors in Water Pollutants Monitoring: Role of Material*, 43-62.

Malik, M., Chan, K. H., & Azimi, G. (2021). Quantification of nickel, cobalt, and manganese concentration using ultraviolet-visible spectroscopy. *RSC Advances*, **11**(45), 28014-28028.

Manobala, T., Shukla, S. K., Rao, T. S., & Kumar, M. D. (2021). Kinetic modelling of the uranium biosorption by *Deinococcus radiodurans* biofilm. *Chemosphere*, **269**, 128722.

Mekonnen, E., Yitbarek, M., & Soreta, T. R. (2015). Kinetic and thermodynamic studies of the adsorption of Cr (VI) onto some selected local adsorbents. *South African Journal of Chemistry*, **68**, 45-52.

Mishra, S., Gnanasoundari, J., Rajeev, R., Desigan, N., Velavendan, P., Venkatesan, K. A., & Ananthasivan, K. (2023). Wiped film evaporator with a roller wiper and an internally mounted condenser for the recovery of TBP and n-DD from degraded PUREX solvent. *Chemical Engineering Research and Design*, **192**, 223-238.

Mitra, A., & Zaman, S. (2015). *Blue Carbon Reservoir of The Blue Planet* (pp. 1-299). New Delhi: Springer.

Moyo, M. (2013). Bioremediation of lead (II) from polluted wastewaters employing sulphuric acid treated maize tassel biomass. *American Journal of Analytical Chemistry*, **4**(12), 689.

Mpatani, F. M., Han, R., Aryee, A. A., Kani, A. N., Li, Z., & Qu, L. (2021). Adsorption performance of modified agricultural waste materials for removal of emerging micro-contaminant bisphenol A: a comprehensive review. *Science of The Total Environment*, **780**, 146629.

Nagul, E. A., McKelvie, I. D., Worsfold, P., & Kolev, S. D. (2015). The molybdenum blue reaction for the determination of orthophosphate revisited: Opening the black box. *Analytica Chimica Acta*, **890**, 60-82.

Nguyen, T. A. H., Ngo, H. H., Guo, W. S., Nguyen, T. V., Zhang, J., Liang, S., Chen, S.S. & Nguyen, N. C. (2014). A comparative study on different metal loaded soybean milk by-product ‘okara’for biosorption of phosphorus from aqueous solution. *Bioresource Technology*, **169**, 291-298.

Nguyen, T. A. H., Ngo, H. H., Guo, W. S., Nguyen, T. V., Zhang, J., Liang, S., Chen, S.S., & Nguyen, N. C. (2014). A comparative study on different metal loaded

soybean milk by-product ‘okara’for biosorption of phosphorus from aqueous solution. *Bioresource Technology*, **169**, 291-298.

Nguyen, T. A. H., Ngo, H. H., Guo, W. S., Pham, T. Q., Li, F. M., Nguyen, T. V., & Bui, X. T. (2015). Adsorption of phosphate from aqueous solutions and sewage using zirconium loaded okara (ZLO): fixed-bed column study. *Science of The Total Environment*, **523**, 40-49.

Nguyen, T. A. H., Ngo, H. H., Guo, W. S., Zhang, J., Liang, S., & Tung, K. L. (2013). Feasibility of iron loaded ‘okara’for biosorption of phosphorous in aqueous solutions. *Bioresource Technology*, **150**, 42-49.

O’Boyle, S. (2020). Oxygen Depletion in Coastal Waters and the Open Ocean: Hypoxia and Anoxia Cases and Consequences for Biogeochemical Cycling and Marine Life. In *Coastal and Deep Ocean Pollution* (pp. 41-67). CRC Press.

Olatinsu, O. B., Ndukwe-Agu, G. C., & Ozebo, V. C. (2023). Joint geophysical and hydrogeochemical assessment of groundwater quality degradation in coastal aquifer systems at a suburb of Kosofe, Lagos, southwest Nigeria. *Sustainable Water Resources Management*, **9**(1), 19.

Omae, A. L., Solo-Gabriele, H. M., & Townsend, T. G. (2007). A Chemical Stain for Identifying Arsenic-Treated Wood Products. *Journal of wood chemistry and technology*, **27**(3-4), 201-217.

Palansooriya, K. N., Kim, S., Igalavithana, A. D., Hashimoto, Y., Choi, Y. E., Mukhopadhyay, R., & Ok, Y. S. (2021). Fe (III) loaded chitosan-biochar composite fibers for the removal of phosphate from water. *Journal of Hazardous Materials*, **415**, 125464.

Palansooriya, K. N., Kim, S., Igalavithana, A. D., Hashimoto, Y., Choi, Y. E., Mukhopadhyay, R., & Ok, Y. S. (2021). Fe (III) loaded chitosan-biochar composite fibers for the removal of phosphate from water. *Journal of Hazardous Materials*, **415**, 125464.

Pan, J., Gao, B., Song, W., Xu, X., & Yue, Q. (2020). Modified biogas residues as an eco-friendly and easily-recoverable biosorbent for nitrate and phosphate removals from surface water. *Journal of Hazardous Materials*, **382**, 121073.

Pasek, M. A. (2019). Thermodynamics of prebiotic phosphorylation. *Chemical Reviews*, **120**(11), 4690-4706.

Peleka, E. N., & Deliyanni, E. A. (2009). Adsorptive removal of phosphates from aqueous solutions. *Desalination*, **245**(1-3), 357-371.

Piol, M. N., Dickerman, C., Ardanza, M. P., Saralegui, A., & Boeykens, S. P. (2021). Simultaneous removal of chromate and phosphate using different operational combinations for their adsorption on dolomite and banana peel. *Journal of Environmental management*, **288**, 112463.

Pokhrel, M. R., Poudel, B. R., Aryal, R. L., Paudyal, H., & Ghimire, K. N. (2019). Removal and recovery of phosphate from water and wastewater using metal-loaded agricultural waste-based adsorbents: a review. *Journal of Institute of Science and Technology*, **24**(1), 77-89.

Preisner, M., Neverova-Dziopak, E., & Kowalewski, Z. (2021). Mitigation of eutrophication caused by wastewater discharge: A simulation-based approach. *Ambio*, **50**(2), 413-424.

Priyadarshanee, M., & Das, S. (2021). Biosorption and removal of toxic heavy metals by metal tolerating bacteria for bioremediation of metal contamination: A comprehensive review. *Journal of Environmental Chemical Engineering*, **9**(1), 104686.

Qu, J., Akindolie, M. S., Feng, Y., Jiang, Z., Zhang, G., Jiang, Q., Deng, F., Cao, B. & Zhang, Y. (2020). One-pot hydrothermal synthesis of $NaLa(CO_3)_2$ decorated magnetic biochar for efficient phosphate removal from water: kinetics, isotherms, thermodynamics, mechanisms and reusability exploration. *Chemical Engineering Journal*, **394**, 124915.

Rathod, M., Mody, K., & Basha, S. (2014). Efficient removal of phosphate from aqueous solutions by red seaweed, *Kappaphycus alverezii*. *Journal of Cleaner Production*, **84**, 484-493.

Riahi, K., Thayer, B. B., Mammou, A. B., Ammar, A. B., & Jaafoura, M. H. (2009). Biosorption characteristics of phosphates from aqueous solution onto *Phoenix dactylifera L.* date palm fibers. *Journal of Hazardous Materials*, **170**(2-3), 511-519.

Riederer, M. (1990). Estimating partitioning and transport of organic chemicals in the foliage/atmosphere system: discussion of a fugacity-based model. *Environmental science & technology*, **24**(6), 829-837.

Rihal, V., Khan, H., Kaur, A., & Singh, T. G. (2022). Vitamin D as therapeutic modulator in cerebrovascular diseases: a mechanistic perspectives. *Critical Reviews in Food Science and Nutrition*, 1-23.

Rout, P. R., Bhunia, P., & Dash, R. R. (2014). Modeling isotherms, kinetics and understanding the mechanism of phosphate adsorption onto a solid waste: ground burnt patties. *Journal of Environmental Chemical Engineering*, **2**(3), 1331-1342.

Ruan, W., Cai, H., Xu, X., Man, Y., Wang, R., Tai, Y., Chen, Z., Vymazal, J., Chen, J., Yang, Y. & Zhang, X. (2021). Efficiency and plant indication of nitrogen and phosphorus removal in constructed wetlands: A field-scale study in a frost-free area. *Science of The Total Environment*, **799**, 149301.

Sahu, N., Singh, J., & Koduru, J. R. (2021). Removal of arsenic from aqueous solution by novel iron and iron–zirconium modified activated carbon derived from chemical carbonization of *Tectona grandis* sawdust: Isotherm, kinetic, thermodynamic and breakthrough curve modelling. *Environmental Research*, 111431.

Salam, K. A. (2019). Towards sustainable development of microalgal biosorption for treating effluents containing heavy metals. *Biofuel Research Journal*, **6**(2), 948.

Saleh, A. A. S., Ibrahim, N., Awang, N. R., & Akbar, N. A. (2021). Characteristics study of ammonia-n and phosphorus in sewage wastewater effluent: a case study of Alkhumrah, Jeddah Wastewater Treatment Plant. In *IOP Conference Series: Earth and Environmental Science* (Vol. **842**, No. 1, p. 012034). IOP Publishing.

Saravanan, A., Kumar, P. S., Hemavathy, R. V., Jeevanantham, S., Harikumar, P., Priyanka, G., & Devakirubai, D. R. A. (2022). A comprehensive review on sources, analysis and toxicity of environmental pollutants and its removal methods from water environment. *Science of The Total Environment*, **812**, 152456.

Schatkoski, V. M., do Amaral Montanheiro, T. L., de Menezes, B. R. C., Pereira, R. M., Rodrigues, K. F., Ribas, R. G., & Thim, G. P. (2021). Current advances

concerning the most cited metal ions doped bioceramics and silicate-based bioactive glasses for bone tissue engineering. *Ceramics International*, **47**(3), 2999-3012.

Schnurr, M. A., Addison, L., & Mujabi-Mujuzi, S. (2020). Limits to biofortification: farmer perspectives on a vitamin A enriched Banana in Uganda. *The Journal of Peasant Studies*, **47**(2), 326-345.

Shin, E. W., Karthikeyan, K. G., & Tshabalala, M. A. (2007). Adsorption mechanism of cadmium on juniper bark and wood. *Bioresource Technology*, **98**(3), 588-594.

Shrestha, A., Poudel, B. R., Silwal, M., & Pokhrel, M. R. (2018). Adsorptive removal of phosphate onto iron loaded *Litchi chinensis* seed waste. *Journal of Institute of Science and Technology*, **23**(1), 81-87.

Slocombe, S. P., Zuniga-Burgos, T., Chu, L., Wood, N. J., Camargo-Valero, M. A., & Baker, A. (2020). Fixing the broken phosphorus cycle: wastewater remediation by microalgal polyphosphates. *Frontiers in Plant Science*, **11**, 982.

Sun, F. Y., Wang, X. M., & Li, X. Y. (2013). An innovative membrane bioreactor (MBR) system for simultaneous nitrogen and phosphorus removal. *Process Biochemistry*, **48**(11), 1749-1756.

Thangavelu, K. P., Tiwari, B., Kerry, J. P., McDonnell, C. K., & Álvarez, C. (2022). Phosphate replacing potential of apple pomace and coffee silver skin in Irish breakfast sausage using a mixture design approach. *Meat Science*, **185**, 108722.

Thirunavukkarasu, A., Nithya, R., & Sivashankar, R. (2021). Continuous fixed-bed biosorption process: A review. *Chemical Engineering Journal Advances*, **8**, 100188.

Thongsamer, T., Vinitnantharat, S., Pinisakul, A., & Werner, D. (2022). Chitosan impregnation of coconut husk biochar pellets improves their nutrient removal from eutrophic surface water. *Sustainable Environment Research*, **32**(1), 1-19.

Tiessen, H. (2008). *Phosphorus in The Global Environment* (pp. 1-7). Springer Netherlands.

Tripathi, A., & Ranjan, M. R. (2015). Heavy metal removal from wastewater using low cost adsorbents. *Journal of Bioremediation & Biodegradation*, **6**(6), 315.

Turowski, P. N., Armstrong, W. H., Liu, S., Brown, S. N., & Lippard, S. J. (1994). Synthesis and characterization of hydroxo-bridged diiron (III) complexes containing carboxylate or phosphate ester bridges: comparisons to diiron (III) proteins. *Inorganic Chemistry*, **33**(4), 636-645.

Vikrant, K., Kim, K. H., Ok, Y. S., Tsang, D. C., Tsang, Y. F., Giri, B. S., & Singh, R. S. (2018). Engineered/designer biochar for the removal of phosphate in water and wastewater. *Science of the Total Environment*, **616**, 1242-1260.

Wang, R., Liang, R., Dai, T., Chen, J., Shuai, X., & Liu, C. (2019). Pectin-based adsorbents for heavy metal ions: A review. *Trends in Food Science & Technology*, ***91***, 319-329.

Wang, X., Liu, Z., Liu, J., Huo, M., Huo, H., & Yang, W. (2015). Removing phosphorus from aqueous solutions using lanthanum modified pine needles. *PLoS One*, **10**(12), e0142700.

Wu, Y., Zhang, S., Guo, X., & Huang, H. (2008). Adsorption of chromium (III) on lignin. *Bioresource Technology*, **99**(16), 7709-7715.

Xia, Y., Zhang, M., Tsang, D. C., Geng, N., Lu, D., Zhu, L., Igalavithana, A.D., Dissanayake, P.D., Rinklebe, J., Yang, X., & Ok, Y. S. (2020). Recent advances in control technologies for non-point source pollution with nitrogen and phosphorous from agricultural runoff: current practices and future prospects. *Applied Biological Chemistry*, **63**(1), 1-13.

Xu, X., Gao, B., Wang, W., Yue, Q., Wang, Y., & Ni, S. (2009). Adsorption of phosphate from aqueous solutions onto modified wheat residue: characteristics, kinetic and column studies. *Colloids and Surfaces B: Biointerfaces*, **70**(1), 46-52.

Yaashikaa, P. R., Kumar, P. S., Saravanan, A., & Vo, D. V. N. (2021). Advances in biosorbents for removal of environmental pollutants: A review on pretreatment, removal mechanism and future outlook. *Journal of Hazardous Materials*, **420**, 126596.

Ye, H., Chen, F., Sheng, Y., Sheng, G., & Fu, J. (2006). Adsorption of phosphate from aqueous solution onto modified palygorskites. *Separation and Purification Technology*, **50**(3), 283-290.

Zeitoun, R., & Biswas, A. (2020). Potentiometric determination of phosphate using cobalt: A review. *Journal of The Electrochemical Society*, **167**(12), 127507.

Zhang, H., Zhu, S., Yang, J., Ma, A., & Chen, W. (2021). Enhanced removal efficiency of heavy metal ions by assembling phytic acid on polyamide nanofiltration membrane. *Journal of Membrane Science*, **636**, 119591.

Zhang, L. M., Silvano, E., Rihtman, B., Aguilo-Ferretjans, M., Han, B., Shi, W., & Chen, Y. (2022). Biochemical mechanism of phosphorus limitation impairing nitrogen fixation in diazotrophic bacterium *Klebsiella variicola* W12. *Journal of Sustainable Agriculture and Environment*, **1**(2), 108-117.

Zhang, L., Liu, J., & Guo, X. (2018). Investigation on mechanism of phosphate removal on carbonized sludge adsorbent. *Journal of Environmental Sciences*, **64**, 335-344.

Zhao, Y., Zhang, L. Y., Ni, F., Xi, B., Xia, X., Peng, X., & Luan, Z. (2011). Evaluation of a novel composite inorganic coagulant prepared by red mud for phosphate removal. *Desalination*, **273**(2-3), 414-420.

Zhou, K., Wu, B., Su, L., Xin, W., & Chai, X. (2018). Enhanced phosphate removal using nanostructured hydrated ferric-zirconium binary oxide confined in a polymeric anion exchanger. *Chemical Engineering Journal*, **345**, 640-647.

.

APPENDIX

RBP with $Ca(OH)_2$

Different pH maintained

Oven used for drying RBP, SBP and Fe(III)-SBP

Filtration after biosorption